



# Ultra-compact micro structured palladium membrane reactors for hydrogen production

Roland Dittmeyer

*Director, Institute for Micro Process Engineering (IMVT), Karlsruhe Institute of Technology (KIT), Karlsruhe, Germany*





1. Introduction – Micro structured membrane reactors for hydrogen production
2. On-site steam methane reforming – The  $\mu$ -Enhancer
3. Dehydrogenation of liquid organic hydrogen carriers – The system MCH / TOL
4. Simplified modeling of a micro channel membrane reactor with wall-coated catalyst
  1. Derivation of the governing equations
  2. Flexible solution using Matlab®
5. Some points to remember



# SMALL CAPACITY HYDROGEN SUPPLY AN OPPORTUNITY FOR NEW TECHNOLOGY SUCH AS MEMBRANE REACTORS

Hydrogen supply < 80.000 m<sup>3</sup>/h  
 High pressure and purity (~10-20 bar, >99.999%)

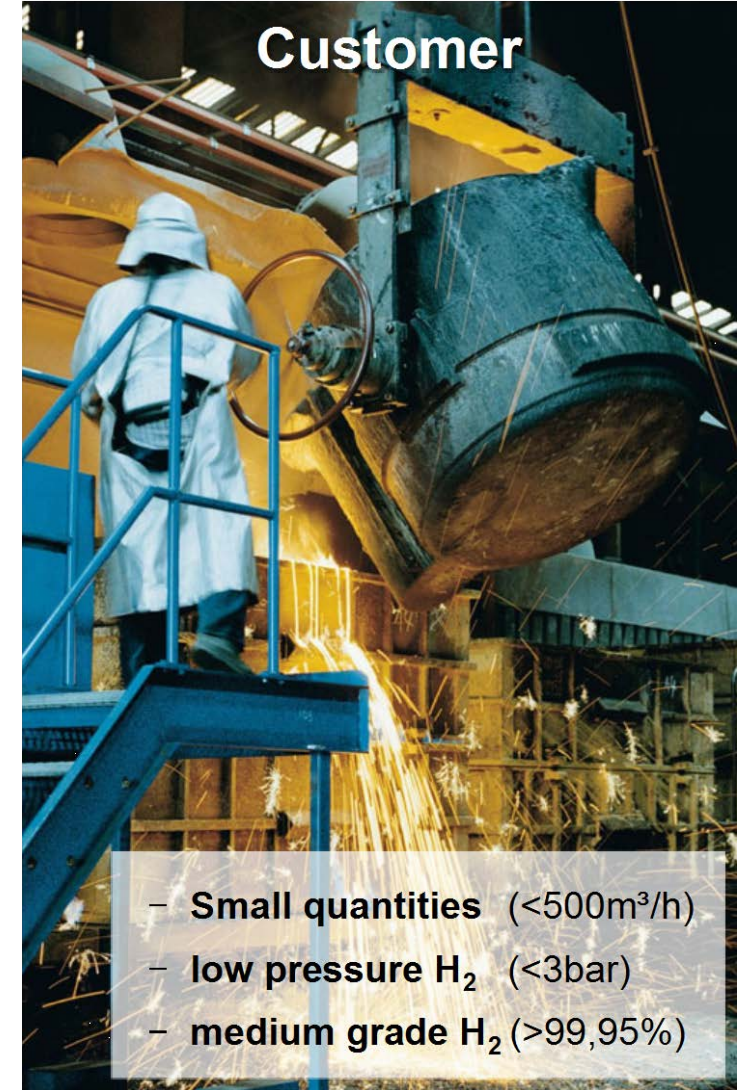


Dittmeyer & Schödel, ICCMR-11, 2013

Hydrogen supply  
 < 500 m<sup>3</sup>/h  
 on-site



**Transport**



**Customer**

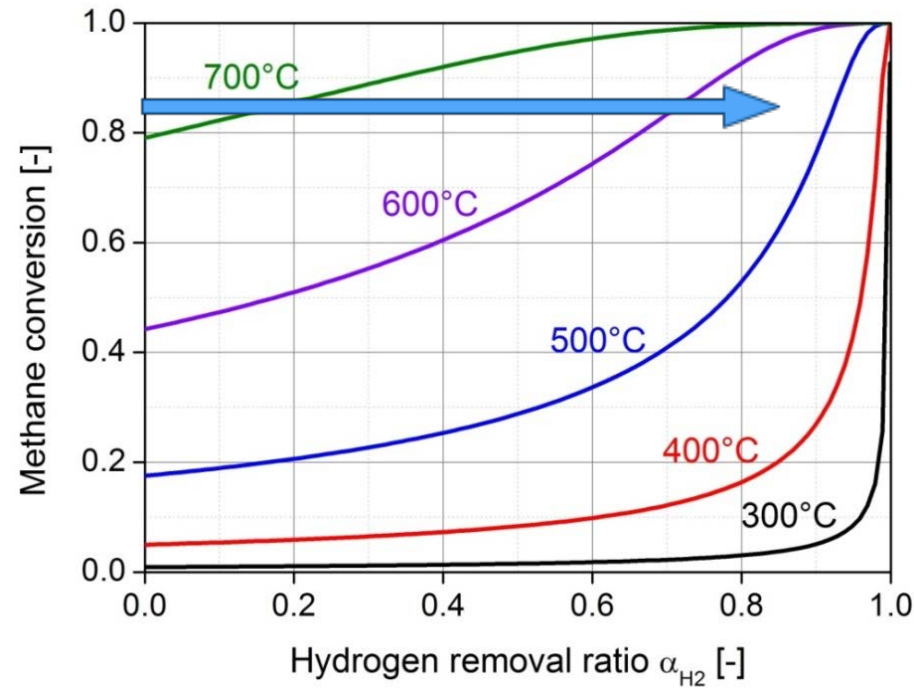
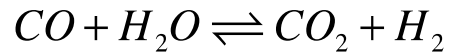
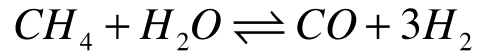
- **Small quantities** (<500m<sup>3</sup>/h)
- **low pressure H<sub>2</sub>** (<3bar)
- **medium grade H<sub>2</sub>** (>99,95%)



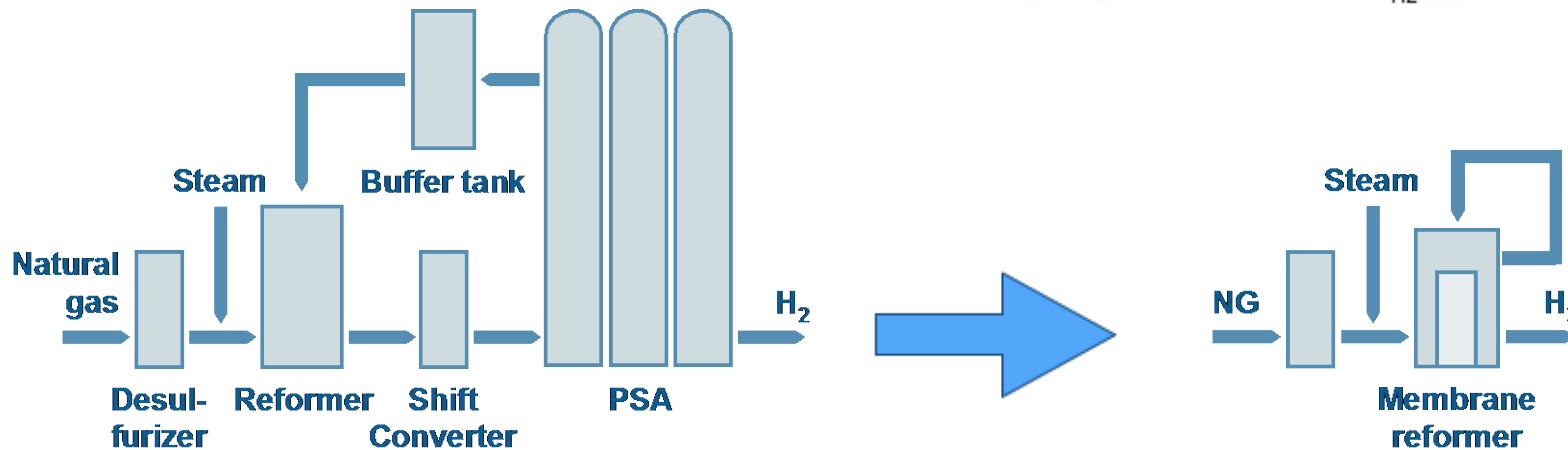
# WHY MEMBRANE REACTORS IN HYDROGEN PRODUCTION?

- Equilibrium shift
- Integrated purification

## Steam methane reforming



**more energy-efficient,  
 lower OPEX**



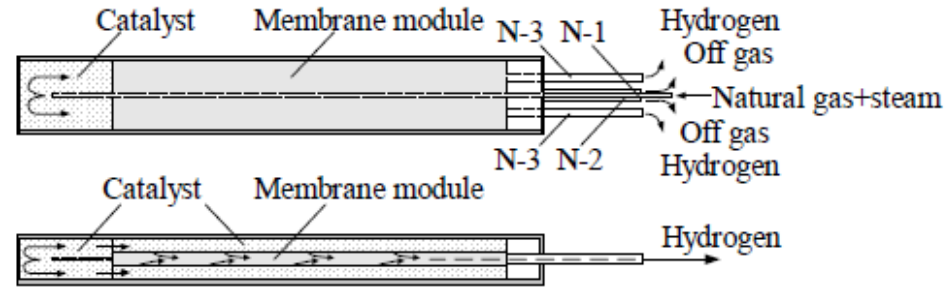
**simpler process,  
 reduced CAPEX**



# BENCHMARK IN MEMBRANE-ASSISTED SMR

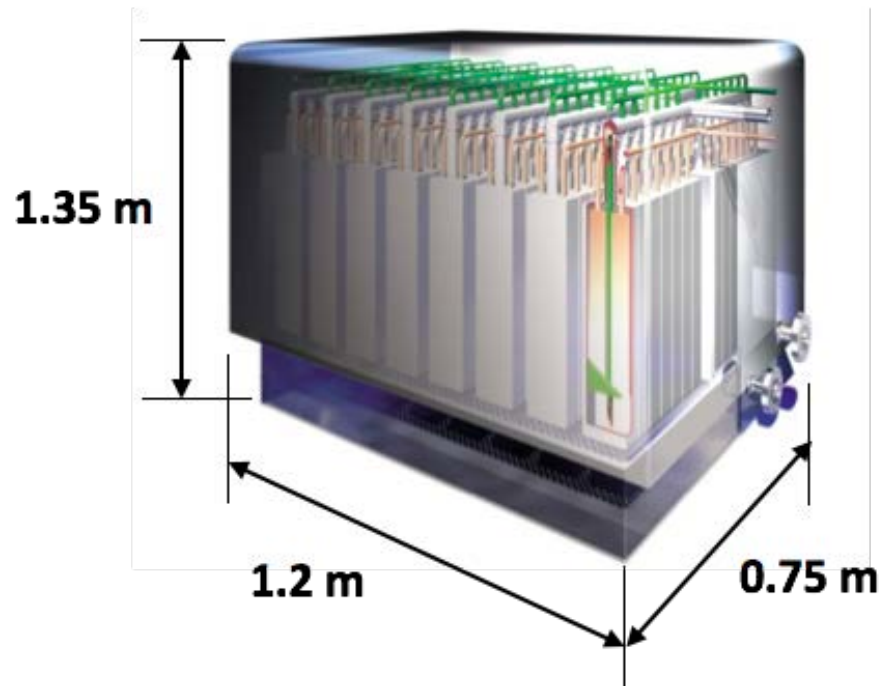
## Tokyo Gas

Modules:



## Modular reformer system:

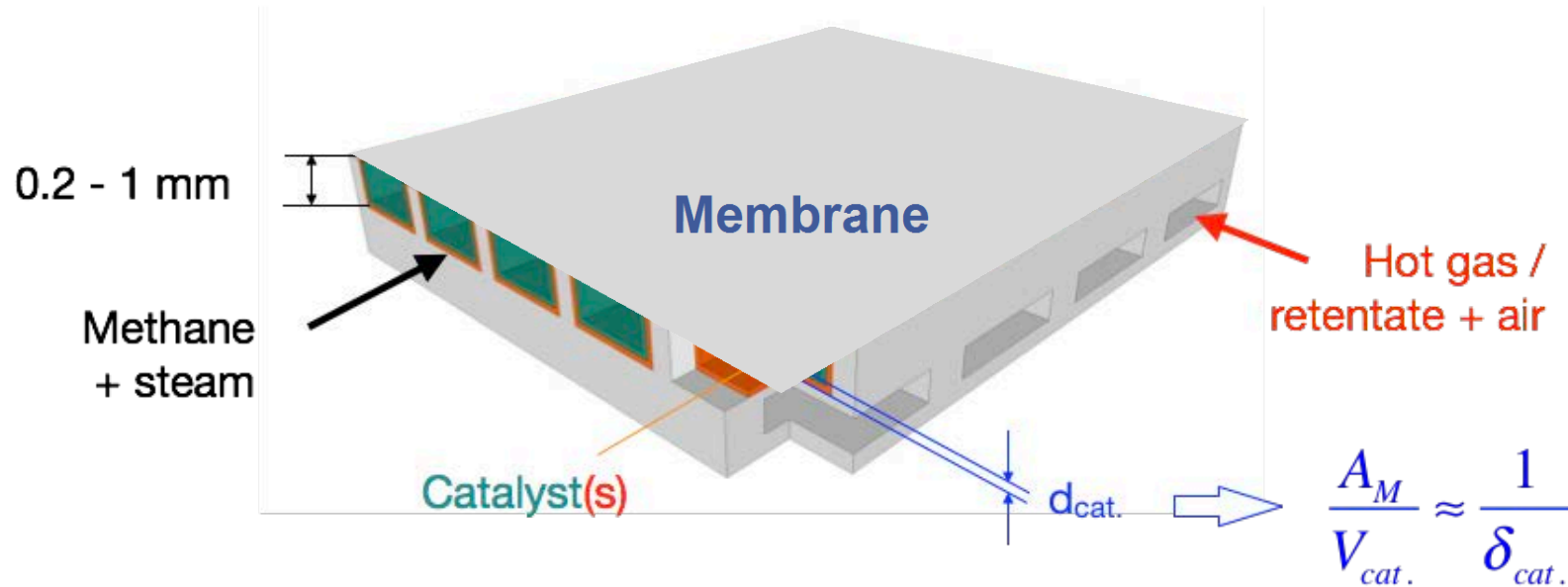
40 m<sub>N</sub><sup>3</sup>/h H<sub>2</sub>



Yasuda et al., 2005, ICCMR-7, Cetraro

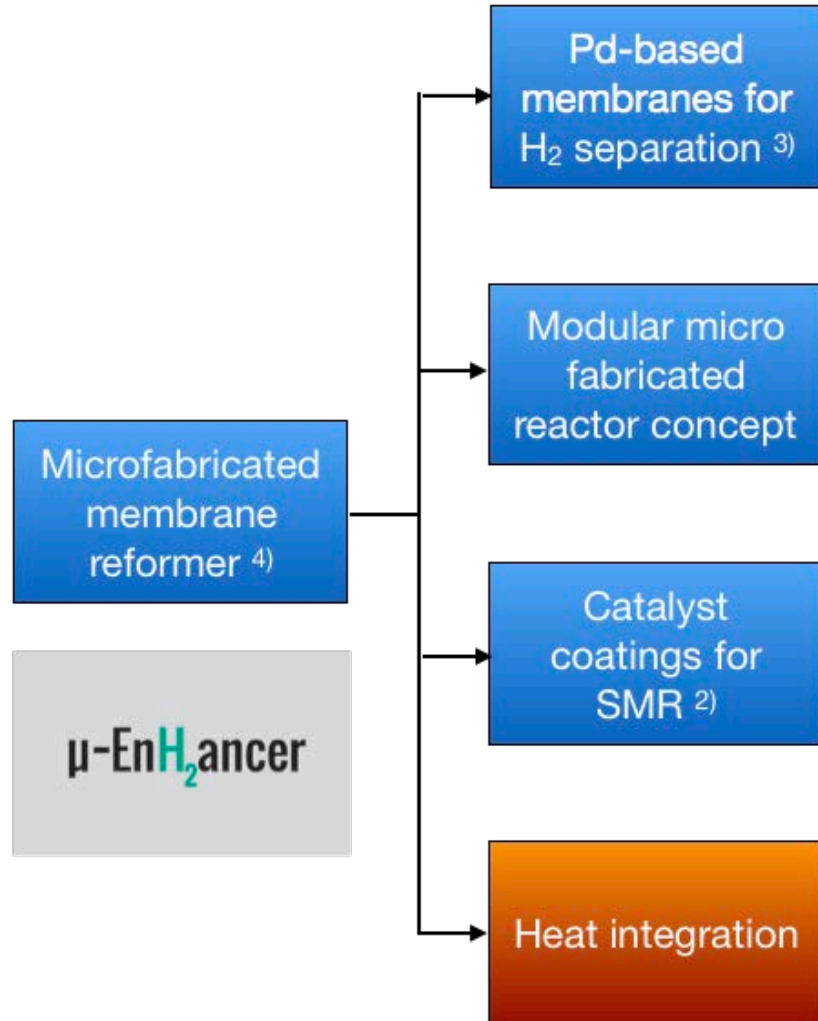


Kurokawa et al., 2010, Demonstration of Highly-Efficient Distributed Hydrogen Production from Natural Gas with CO<sub>2</sub> Capture, WHEC2010, Essen



## Benefits:

- Very large membrane surface area per catalyst volume (ca.  $10^3 - 10^6 \text{ m}^{-1}$ )
- Negligible mass transport resistance towards membrane even for high-flux membranes
- Efficient heating by hot gas or catalytic combustion of retentate with air
- High compactness / low weight / modular plant design



- Preparation of defect-free membranes
- Concepts for thermal and mechanical stability
- Membrane integration by laser welding
- H<sub>2</sub> permeation experiments
- Mass transport performance 3)
- Preparation of Rh/Al<sub>2</sub>O<sub>3</sub> catalysts
- Activity and stability tests
- Reaction kinetics without membrane

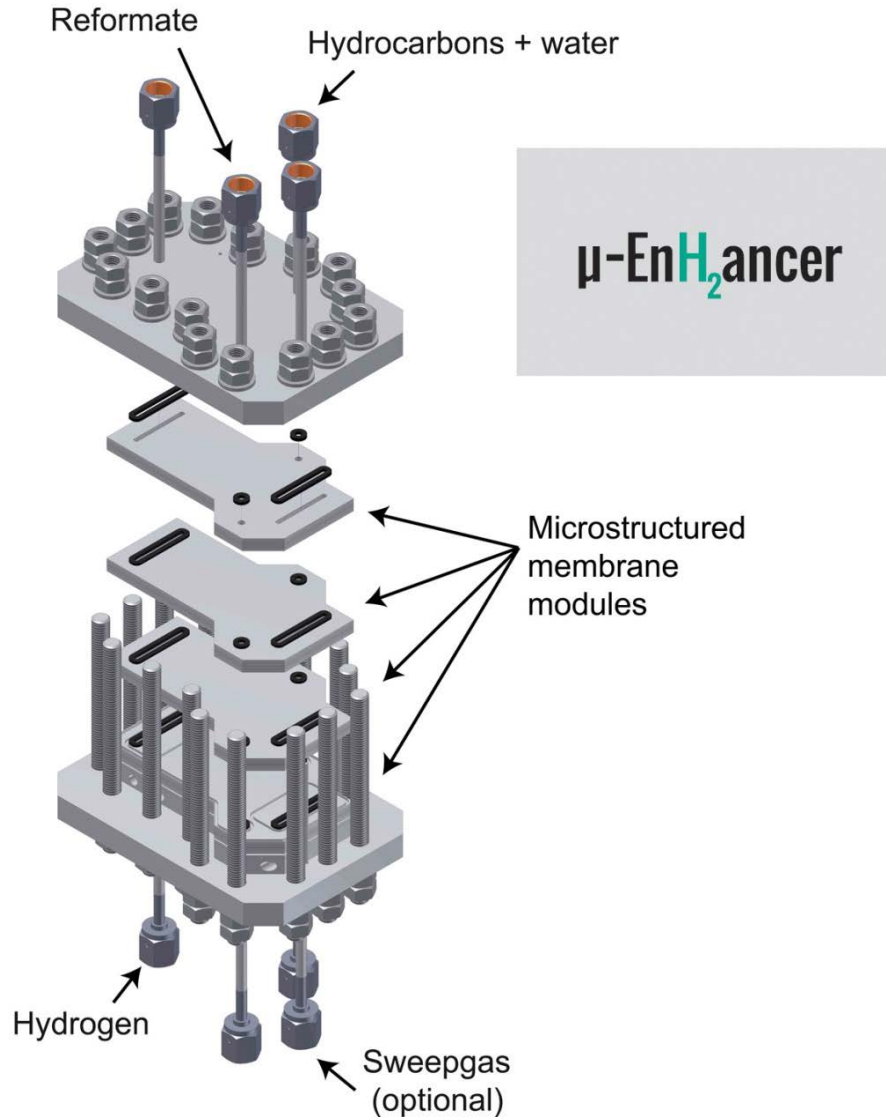
Integration in a technical reactor by laser welding

1) Boeltken et al., CE&P: Process Intensif. 67 (2013) 136-147

2) Lee et al., Appl. Catal. A:Gen. 467 (2013) 69-75

3) Boeltken et al., J. Membr. Sci. 468 (2014) 233-241

4) Boeltken et al., Int. J. Hydr. Energy 41 (2014) 18058-18068



## Pre-reforming stage

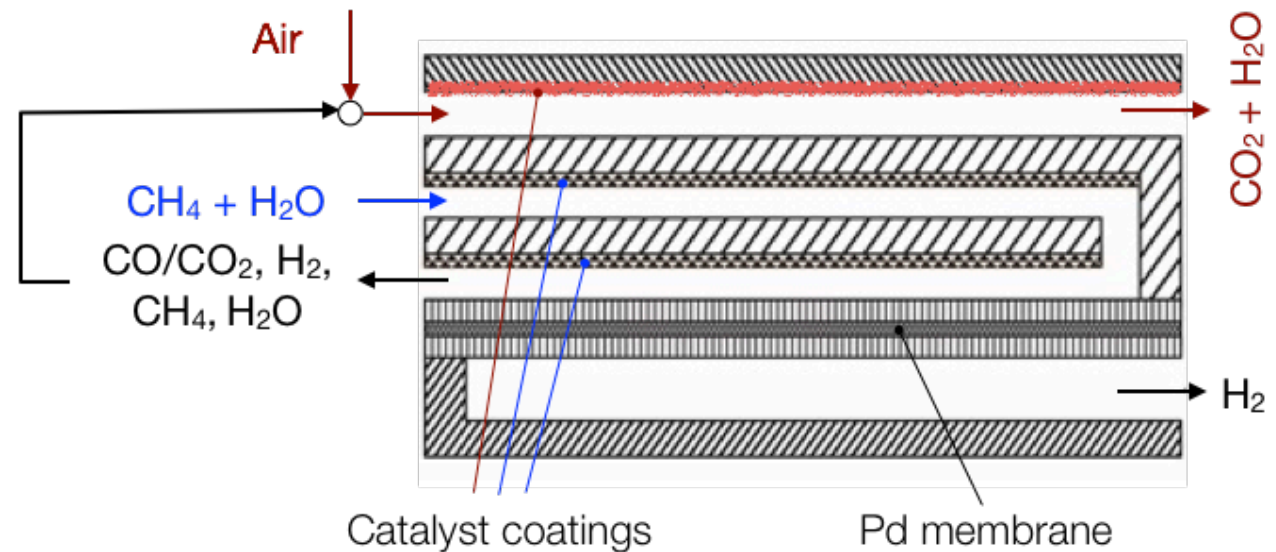
- Cracking of higher hydrocarbons (natural gas)
- Build-up of H<sub>2</sub> partial pressure (by reforming)

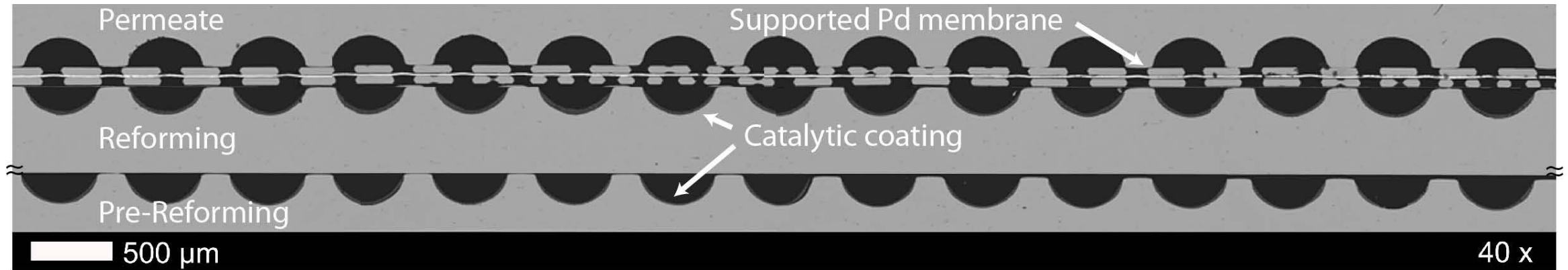
## Reforming stage

- Reforming
- H<sub>2</sub> separation

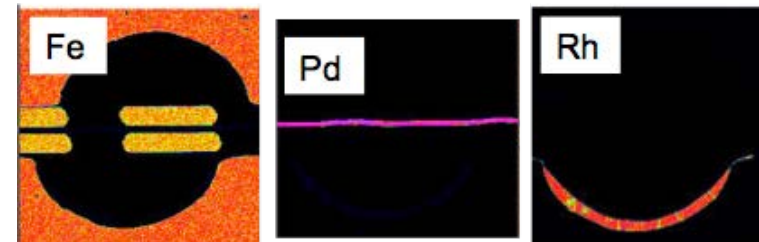
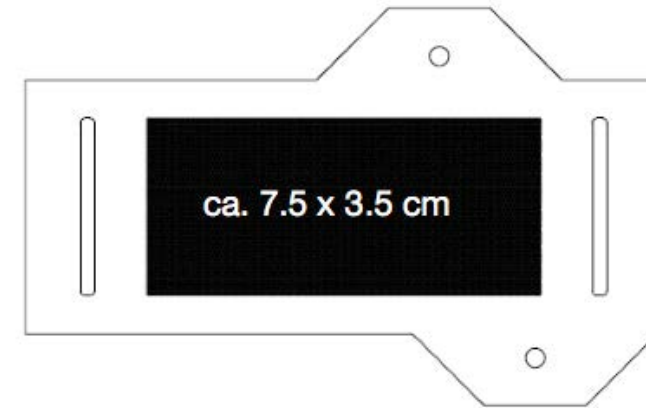
## Retentate combustion zone

- Heat transfer to the reforming zone



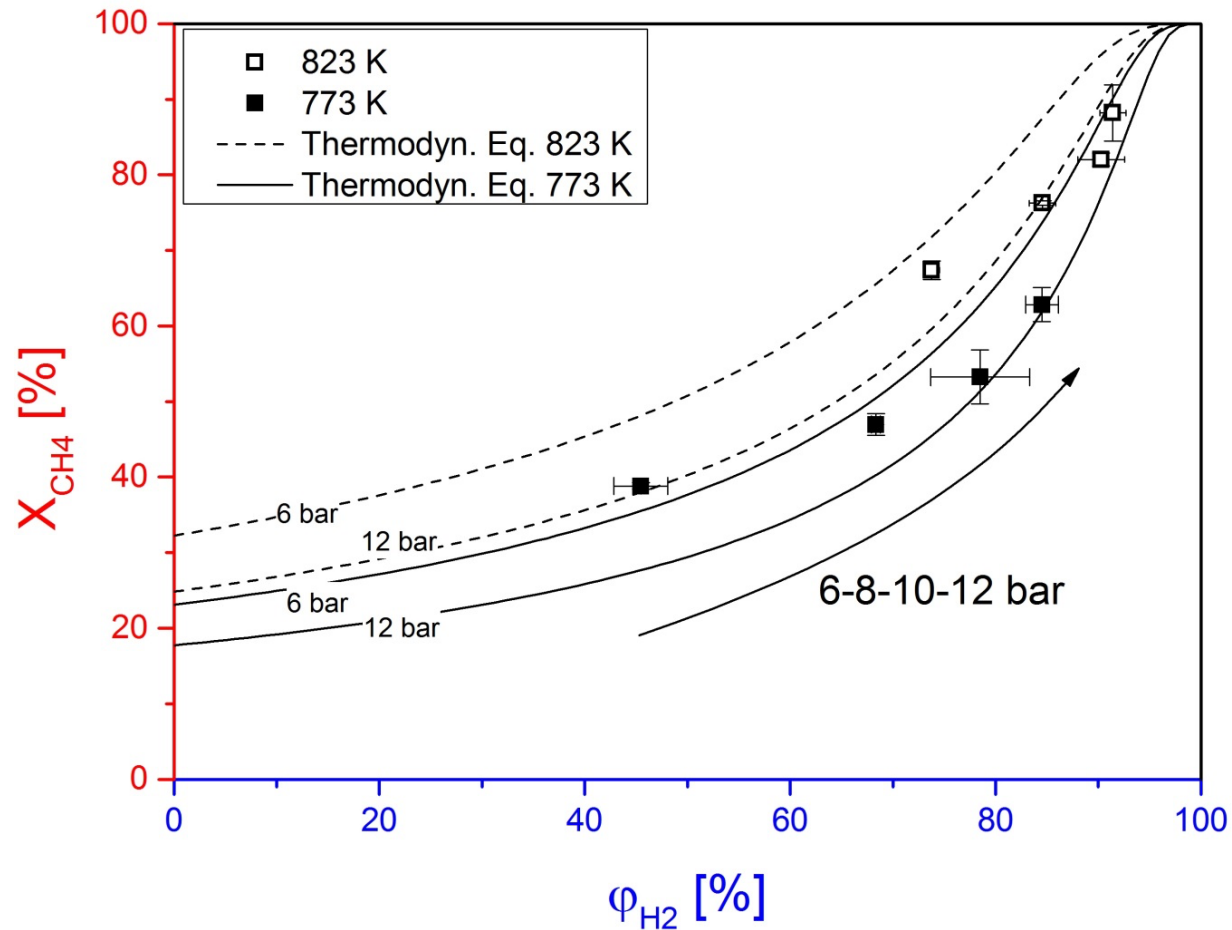


- Modules built from high-temperature corrosion-resistant material (Nicrofer)
- Microchannels by chemical etching (500 x 200 μm)
- Thin palladium foil, i.e., typically 12 μm, sandwiched between two etched microsieves to provide mechanical stability
- Microsieves coated with inorganic diffusion barrier layer to prevent membrane degradation at high temperature
- Catalyst layers by inkjet printing (10-15 μm, 50 mm pre-reforming, 70 mm reforming/membrane)



## SELECTED RESULTS - CONVERSION VERSUS HYDROGEN RECOVERY

Variation of retentate pressure;  $W/F = 0.33 \text{ g}_{\text{Cat}} \text{ h} / \text{mol CH}_4$ ;  $S/C = 3$



Conversion is close to equilibrium considering the fraction of hydrogen removed



Activity of catalyst high enough to respond to H<sub>2</sub> removal



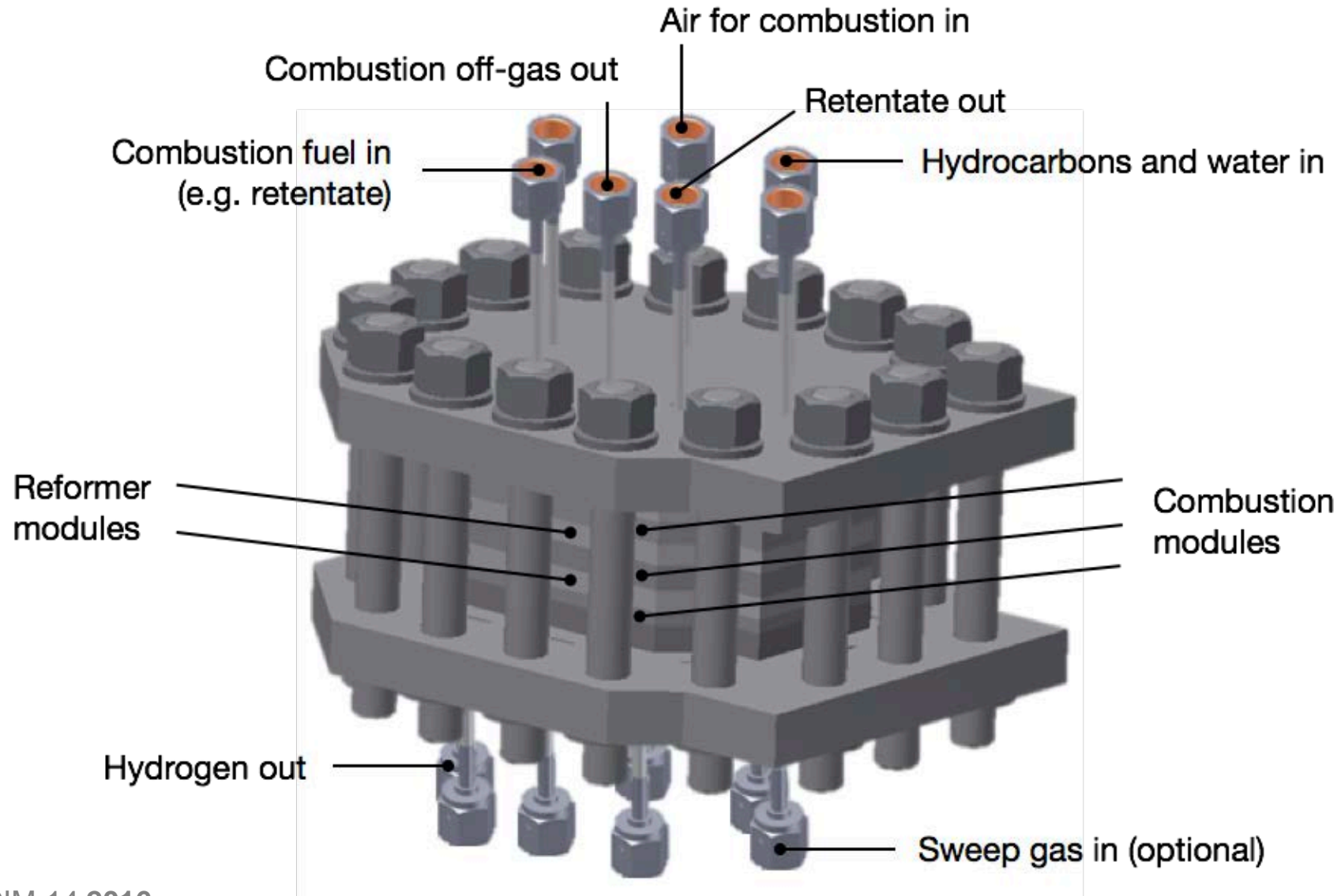
Reference	$S_{Pd}$ [ $\mu\text{m}$ ]	$A_{Pd}$ [ $\text{cm}^2$ ]	Catalyst	T [K]	$\Delta p$ [bar]	$X_{CH_4}$ [%]	$\phi_{H_2}$ [%]	W/F [ $\text{g}_{Cat} \text{h}/\text{mol}_{CH_4}$ ]	$A_{Pd}/V_R$ [ $\text{m}^2/\text{m}^3$ ]	$\dot{V}_{H_2}/V_R$ [ $\text{Nm}^2/(\text{m}^3\text{h})$ ]	$\dot{V}_{H_2}/A_{Pd}$ [ $\text{Nm}^2/(\text{m}^2\text{h})$ ]
Uemiya et al. [4] <sup>1</sup>	20	25.1	Ni-based	773	8 <sup>a</sup>	90	91	64.75	39.3	230	5.9
Tong et al. [6] <sup>2</sup>	8	20	Ni/ $\text{Al}_2\text{O}_3$	823	10 <sup>b</sup>	72	51	74.71	110.1	1289	11.7
Hwang et al. [14] <sup>3</sup>	6.2	33.2	Ni-based	813	20	79	96	n.a.	6.3	58	9.2
Tokyo Gas [15,35] <sup>4</sup>	20	98918.4	Ni-based	823	8.7 <sup>c</sup>	79	n.a.	n.a.	8.1	33	4.1
$\mu$ -EnH <sub>2</sub> ancer [this work]	12.5	26.3 <sup>d</sup>	Rh/ $\text{Al}_2\text{O}_3$	823	11	87	92	0.33	41/66 <sup>e</sup>	472/739 <sup>e</sup>	12.1
<sup>a</sup> Sweep gas 500 ml/min Ar ( $p_{H_2,Perm} = 0.38$ bar). <sup>b</sup> Sweep gas 470 ml/min N <sub>2</sub> . <sup>c</sup> Vacuum ( $p_{H_2,Perm} = 0.4$ bar). <sup>d</sup> Effective membrane area (across the microchannels). <sup>e</sup> Optimized membrane module with thinner microstructured foils.											
<b>Fernandez</b> <sup>5)</sup>	3-5	160	Ni-based	823	1.27	76	20	n.a.	8.0	21	3.0
<b>Mahecho-Botero</b> <sup>6)</sup>	25	1800	Ni-based	823	8.97	80	62.5	n.a.	22.5	125	5.5

- Highest hydrogen production rate per membrane area
- High volumetric hydrogen production rate
- Very compact 41/66 m<sup>-1</sup>

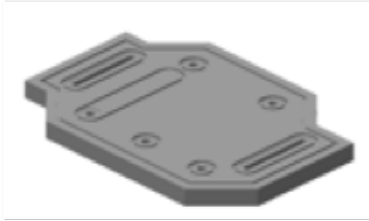
- 1) Uemiya et al., Appl. Catal. **1991**, 67, 223 - 230.
- 2) Tong et al., Catal. Today **2006**, 111, 147 - 152.
- 3) Hwang et al., Int. J. Hydr. Energy **2012**, 37, 6601 - 6607.
- 4) Shirasaki et al., Int. J. Hydr. Energy **2009**, 34, 4482 - 4487.
- 5) Fernandez et al., Int. J. Hydr. Energy **2017**, 42, 13763-13776.
- 6) Mahecha-Botero et al., Chem. Eng. Sci. **2008**, 63, 2752-2762.



# NEW SYSTEM WITH FLUIDIC HEATING ESTABLISHED



**Combustion module  
5 plates, 7.2 mm height**



Gas distribution

Combustion fuel feeding

Combustion fuel distribution  
into plate 4

Oxidant gas feeding and  
combustion

Gas distribution

**Reforming module  
8 plates; 9.4 mm height**



Gas distribution

Gas distribution

Hydrogen removal

Etched micro sieve support

**Palladium foil**

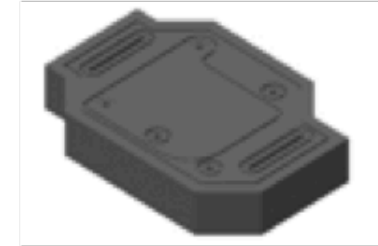
Etched micro sieve support

Reforming zone

Pre-reforming zone

Gas distribution

**Module with integrated reforming and  
combustion zones  
11 plates; 14.4 mm height**



Gas distribution

Combustion fuel feeding and distribution  
into plate 3

Oxidant gas feeding and combustion

Gas distribution

Gas distribution

Permeate gas

Etched micro sieve support

**Palladium foil**

Etched micro sieve support

Reforming zone

Pre-reforming zone

Gas distribution

- all plates fabricated
- microchannel plates awaiting coating with new catalyst
- new porous metal-supported membranes in preparation



## GENERAL INFORMATION

### EXHIBITION

Are you a technology or solution provider and would like to actively contribute to this conference?

The exhibition is an integral part of the IMRET and offers a unique opportunity to promote your technologies, products and services. Equipment suppliers, engineering companies as well as research institutes are invited to participate in the exhibition.



© Karlsruher Messe- & Kongress GmbH

### VENUE

Gartenhalle Karlsruhe  
Festplatz 3  
76137 Karlsruhe / Germany

### ORGANISER

DECHEMA e.V.  
Theodor-Heuss-Allee 25  
60486 Frankfurt am Main / Germany  
www.dechema.de

### CONTACT

Mrs. Chereén Semrau  
Phone: +49 (0)69 7564-651  
Email: semrau@dechema.de



## FIRST ANNOUNCEMENT

21 – 24 October 2018  
Karlsruhe · Germany

## IMRET 2018 15<sup>th</sup> International Conference on Micro Reaction Technology

[www.dechema.de/IMRET2018](http://www.dechema.de/IMRET2018)



© Fraunhofer ICT



SUPPORTED BY:

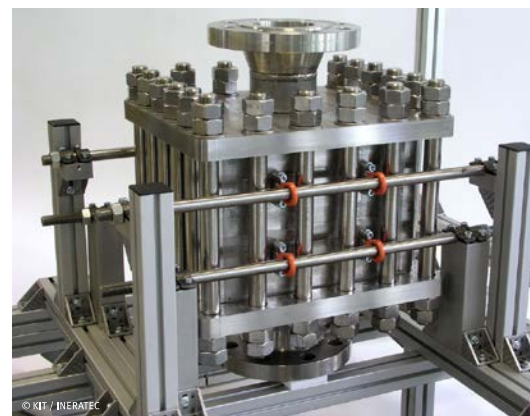
ProcessNet Working Group Microreaction Engineering and  
International Flow Chemistry Society

## INVITATION TO IMRET 15

For its 15<sup>th</sup> edition, the International Conference on Micro Reaction Technology (IMRET) is coming back to where it all began. Since the start of this “place to be” for chemists, chemical engineers and micro systems engineers, the event has demonstrated a variety of new applications in chemical engineering, chemistry, related disciplines like energy supply, and even more different fields such as analytics, life science and medicine. Yet, as each of the involved disciplines has seen amazing progress, the mission of providing an effective platform for exchange is more topical than ever.

IMRET 15 therefore sets out to become once more the place where new developments regarding all facets of micro process engineering and flow chemistry will be jointly discussed for mutual benefit.

IMRET 15 will take place in the city of Karlsruhe from 21 October to 24 October 2018, organised by DECHEMA e.V. with the support of the German ProcessNet Working Group Microreaction Engineering, the IMRET Steering Committee and the International Flow Chemistry Society.



© KIT / INERATEC

## TOPICS / DATES / COMMITTEE

### CONFERENCE TOPICS

- » **Mixing and heat transfer in micro systems**
- » **Reactions and catalysis in flow systems**
- » **Downstream processing**
- » **Modelling/simulation**
- » **Fabrication of micro-structured devices**
- » **Process automation, sensors, digitalization**
- » **Modular plant concepts**
- » **New applications in chemistry, biology, energy etc.**
- » **Industrial implementation**

### IMPORTANT DATES

October 2017	Submission of abstract is open
February 2018	End of abstract submission
April 2018	Notification of acceptance
May 2018	Final programme
21 - 24 October 2018	IMRET 15 takes place

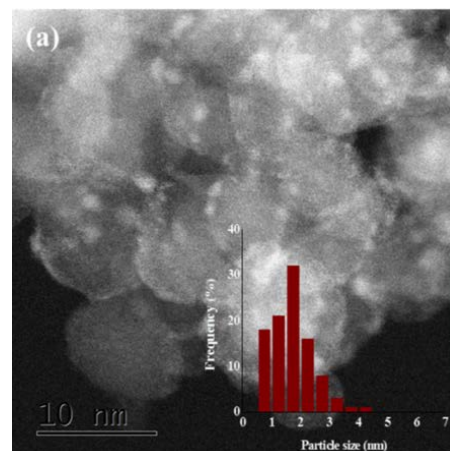
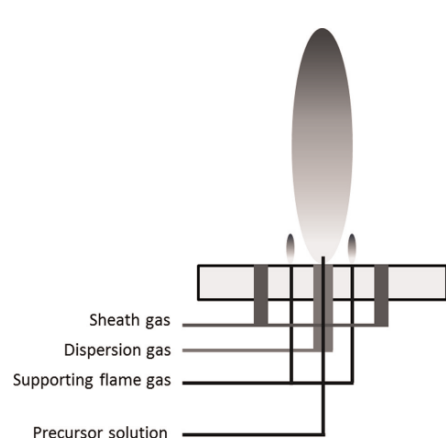
### LOCAL ORGANISING COMMITTEE

<b>Dr. Alexis Bazzanella</b>	DECHEMA e.V.
<b>Prof. Dr. Roland Dittmeyer</b>	KIT, Institute for Micro Process Engineering
<b>Dr. Kerry Gilmore</b>	Max Planck Institute of Colloids and Interfaces
<b>Dr. Christian Holtze</b>	BASF SE
<b>Prof. Dr. Gunther Kolb</b>	Fraunhofer ICT-IMM
<b>Dr. Stefan Loebbecke</b>	Fraunhofer Institute for Chemical Technology ICT

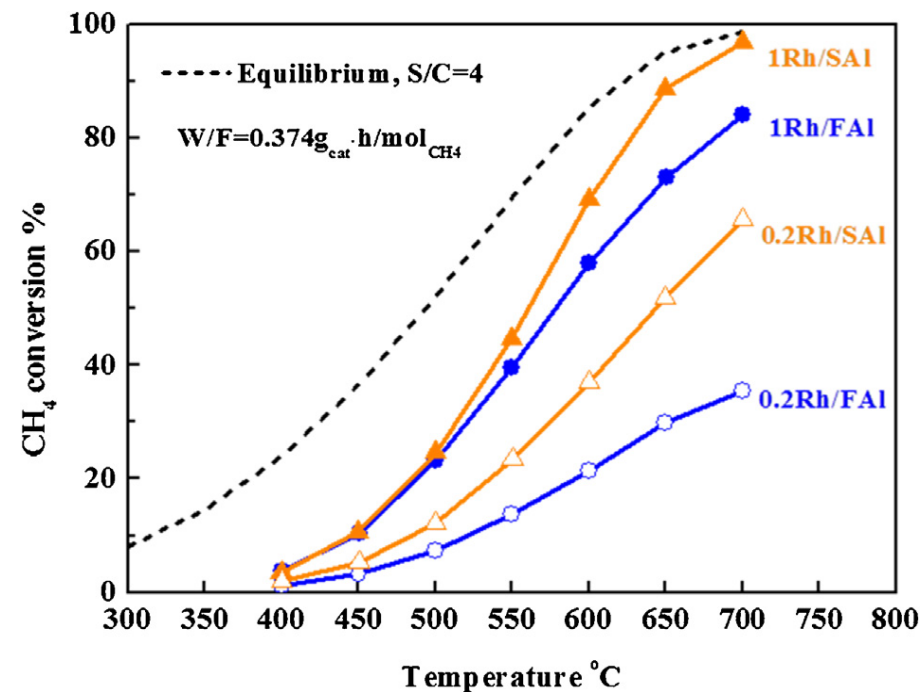
[www.dechema.de/IMRET2018](http://www.dechema.de/IMRET2018)

# RH/AL<sub>2</sub>O<sub>3</sub> CATALYSTS BY FLAME SPRAY PYROLYSIS

Catalyst	Rh loading <sup>a</sup> (%)	H <sub>2</sub> chemisorption results			TEM results	
		Rh active sites (A <sub>chem</sub> ) <sup>b</sup> (μmol/g <sub>cat</sub> )	Rh dispersion <sup>c</sup> (%)	Rh particle size (P <sub>chem</sub> ) <sup>d</sup> (nm)	Rh particle size (P <sub>TEM</sub> ) <sup>e</sup> (nm)	Rh active sites (A <sub>TEM</sub> ) <sup>f</sup> (μmol/g <sub>cat</sub> )
		5Rh/FAI	3.85	174	47	2.4
5Rh/SAI	2.75	117	44	2.5	3.5	90
1Rh/FAI	0.94	69	75	1.5	1.0	105
1Rh/SAI	0.84	59	73	1.5	1.7	53
0.2Rh/FAI	0.20	13	69	1.6	—	—
0.2Rh/SAI	0.20	12	61	1.8	—	—

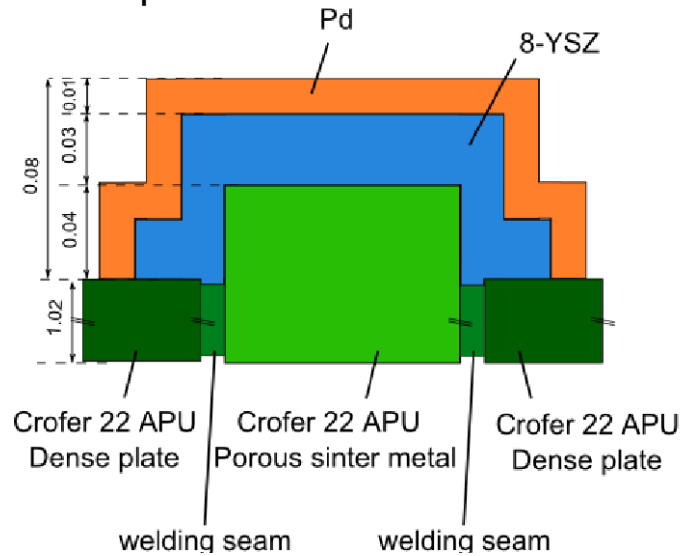


- a Rh loading derived from ICP-OES.
- b From H<sub>2</sub> uptake in chemisorption assuming a stoichiometry of H/Rh = 1.
- c Ratio of active Rh from H<sub>2</sub> chemisorption and Rh content from ICP-OES.
- d From metal dispersion by H<sub>2</sub> chemisorption.
- e From TEM measurements.
- f Derived from TEM results.



In cooperation with Forschungszentrum Jülich (Martin Bram, IEK-1)

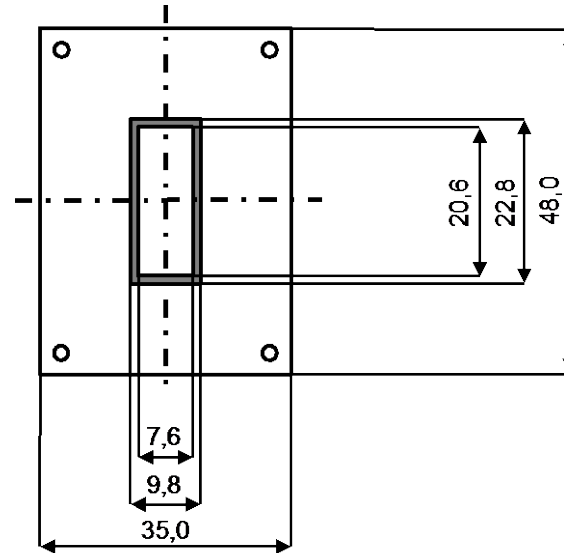
## Concept



- **Pd:** ca. 4 - 12  $\mu\text{m}$  (foil or SPS coating)
- **8-YSZ:** ca. 20 - 40  $\mu\text{m}$
- **Sinter metal:** ca. 1 mm

Dittmeyer et al., ICCMR-13 2017

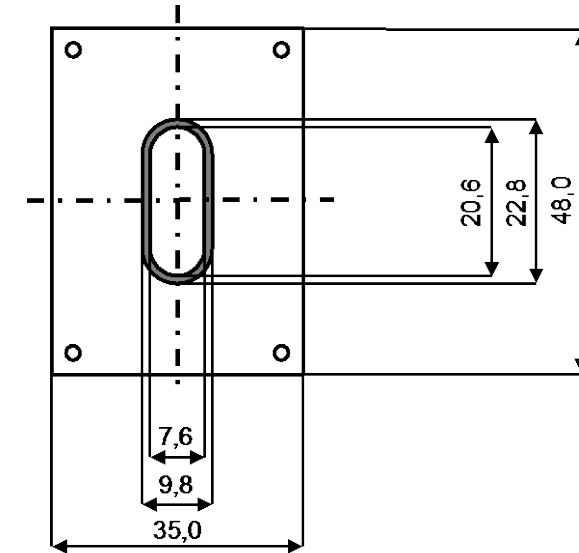
## Test specimen



## Testing unit



Boeltken et al., CE&P 2013, 67,136-147

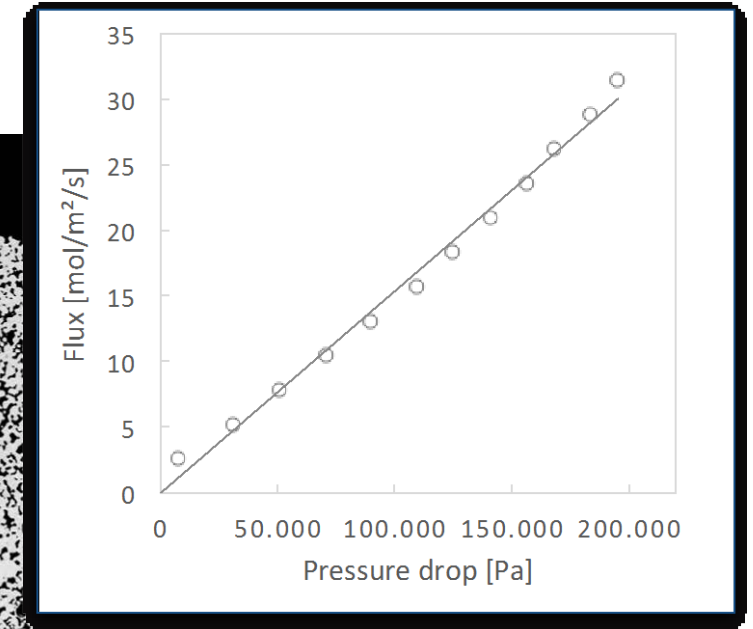
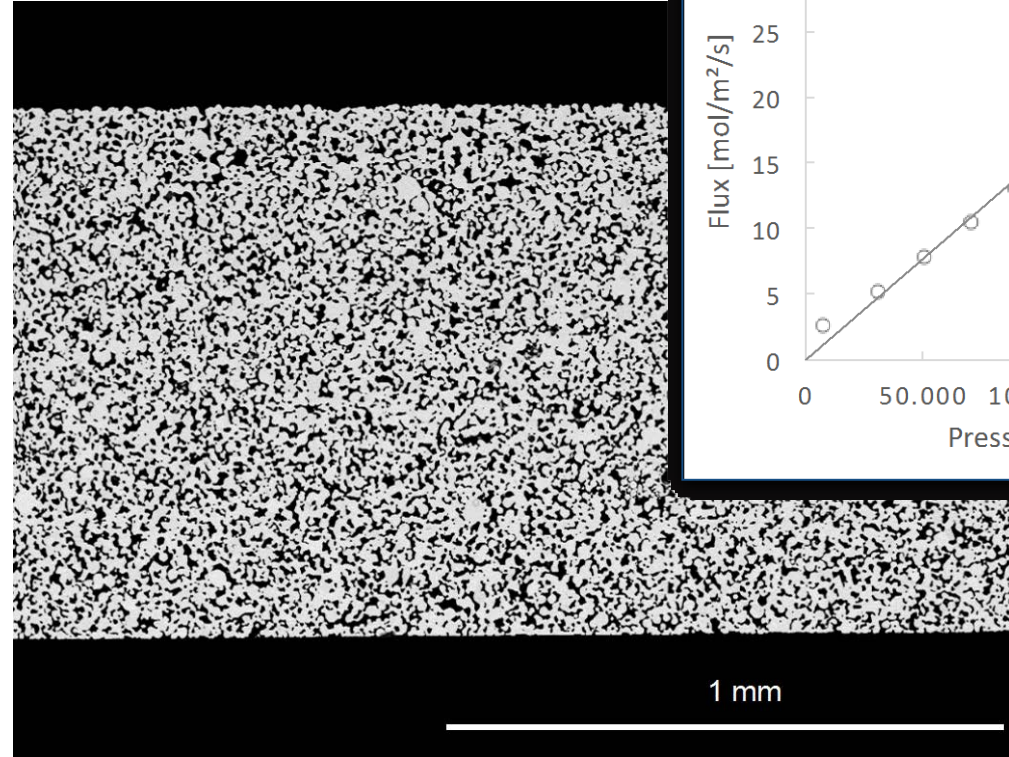
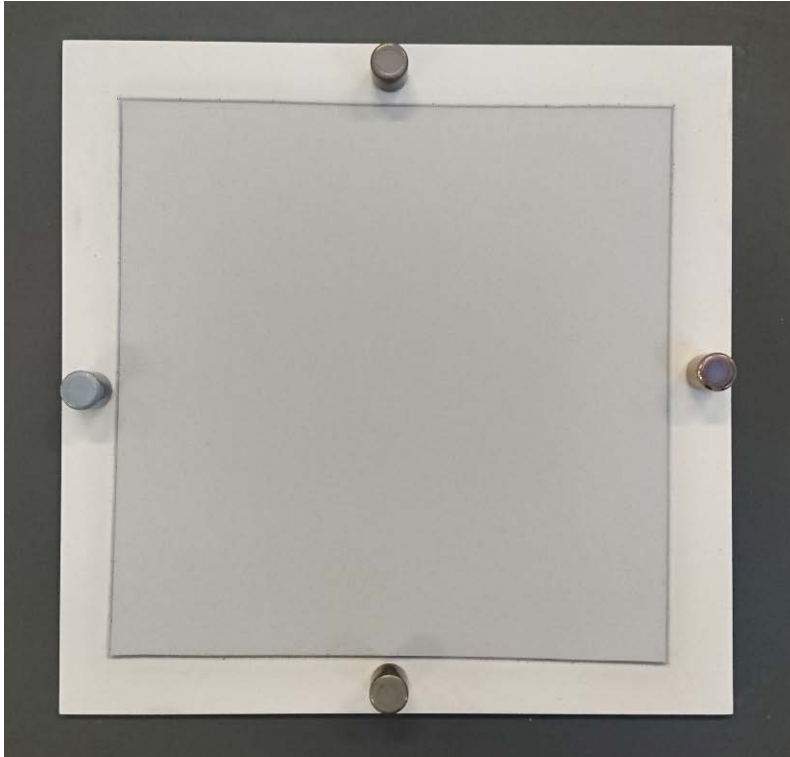


## Transfer to membrane reformer modules



## POROUS SHEETS FROM CROFER 22 APU BY TAPE CASTING / SINTERING

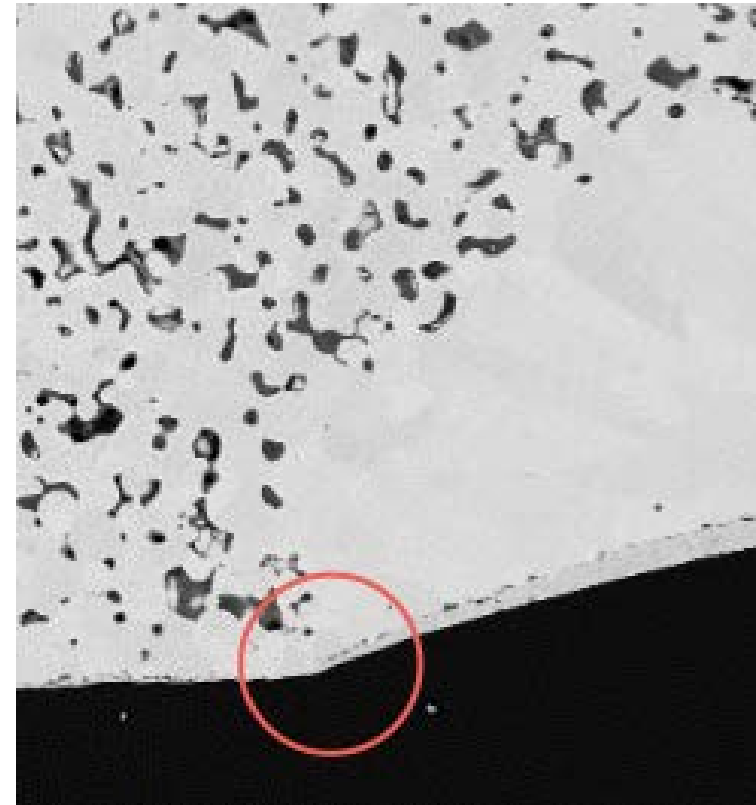
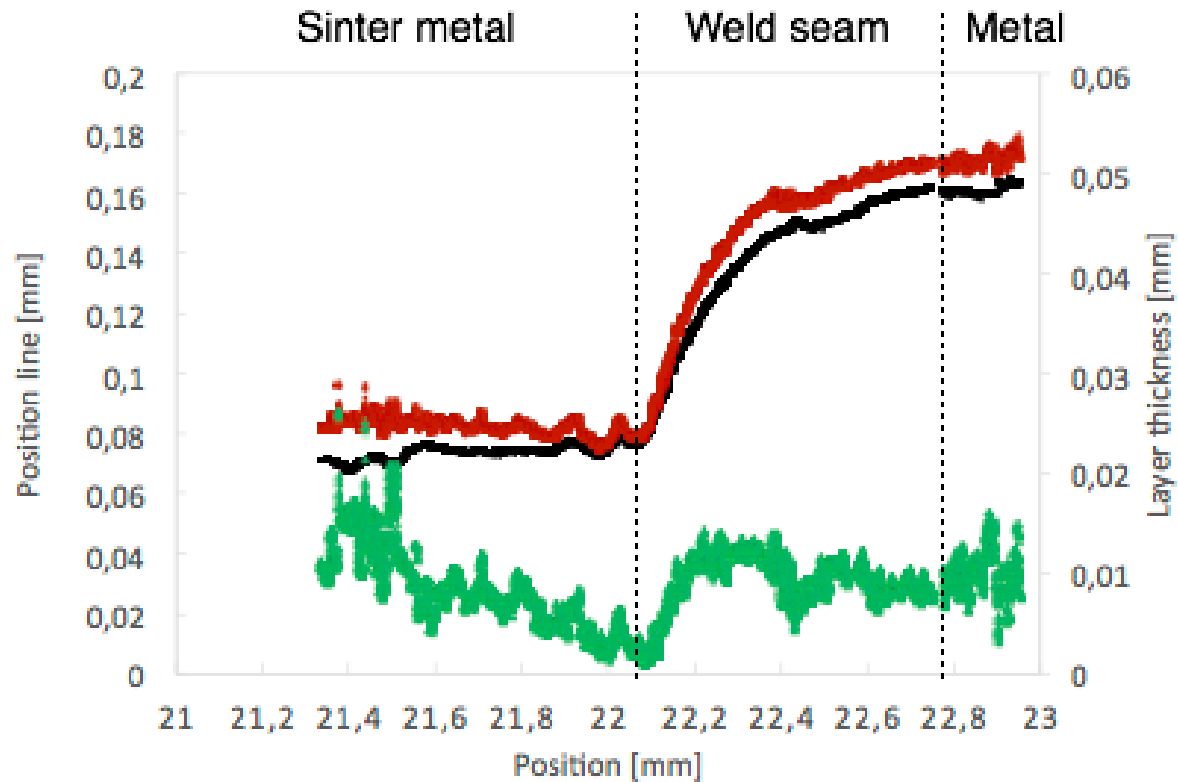
Forschungszentrum Jülich (Martin Bram, IEK-1)



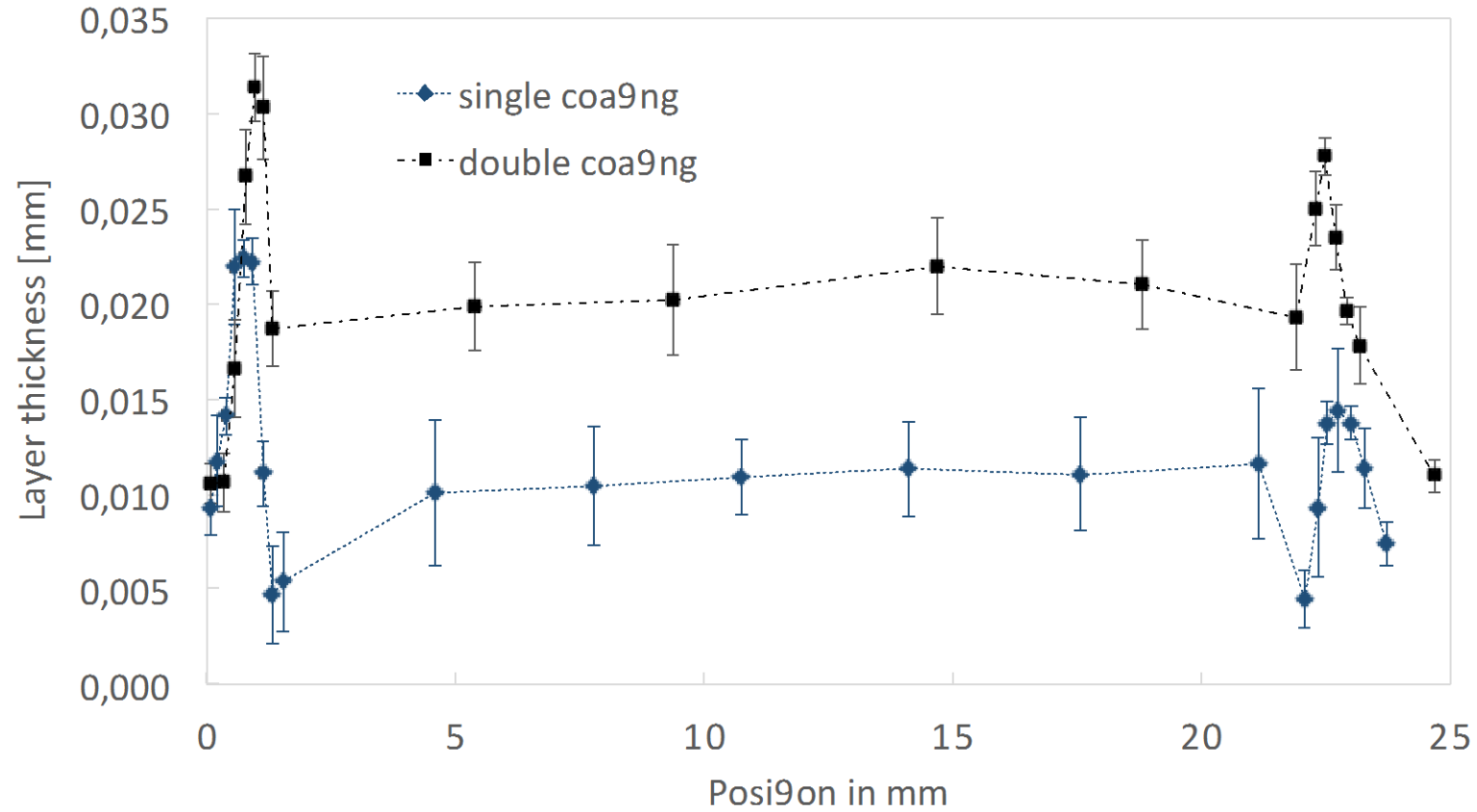
- Porosity:  $27 \pm 4\%$  ( $29.5 \pm 0.9\%$ )
- Thickness:  $1.08 \pm 0.05$  mm

- $N_2$  permeability:  $0.162 \pm 0.003$   $\mu\text{mol}/\text{m}/\text{s}/\text{Pa}$
- $N_2$  permeance:  $1.5 \times 10^{-4}$   $\text{mol}/\text{m}^2/\text{s}/\text{Pa}$

Forschungszentrum Jülich (Martin Bram, IEK-1, Paul Kant, IMVT)



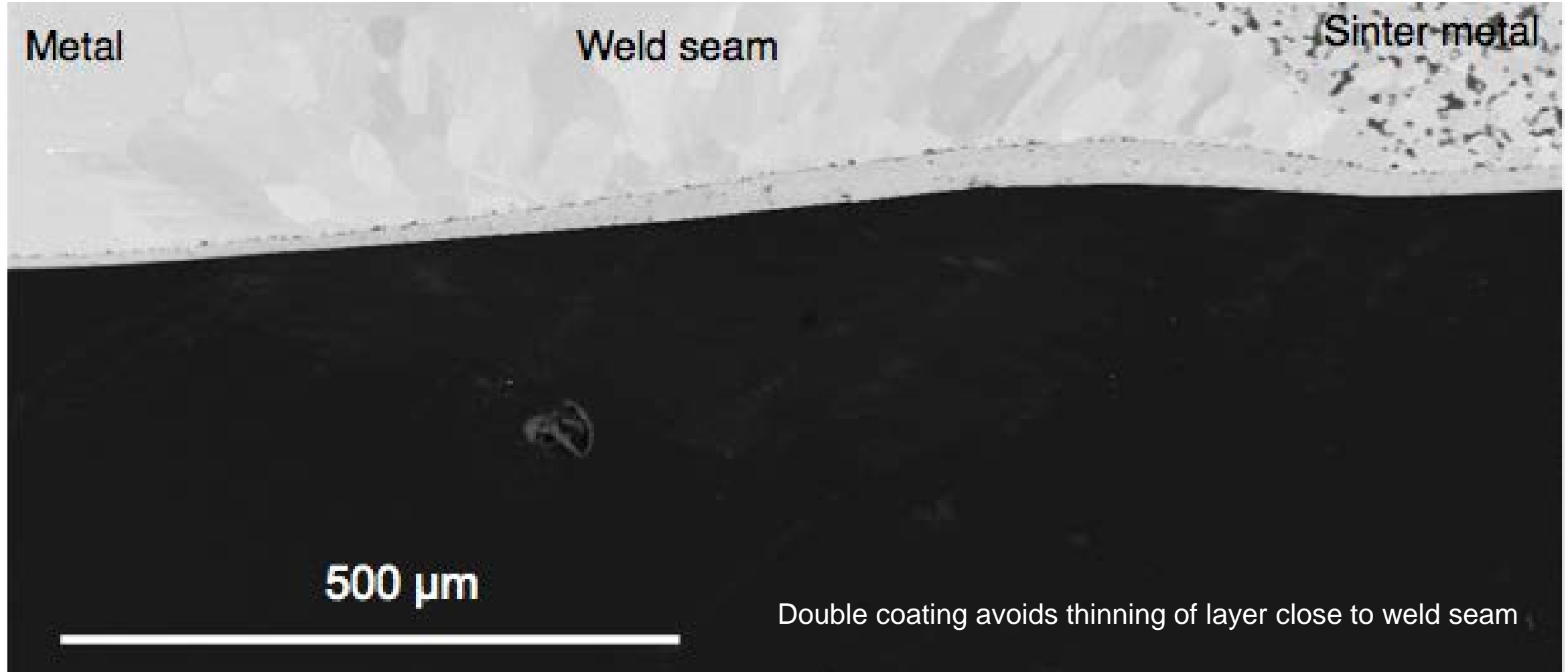
Forschungszentrum Jülich (Martin Bram, IEK-1, Paul Kant, IMVT)



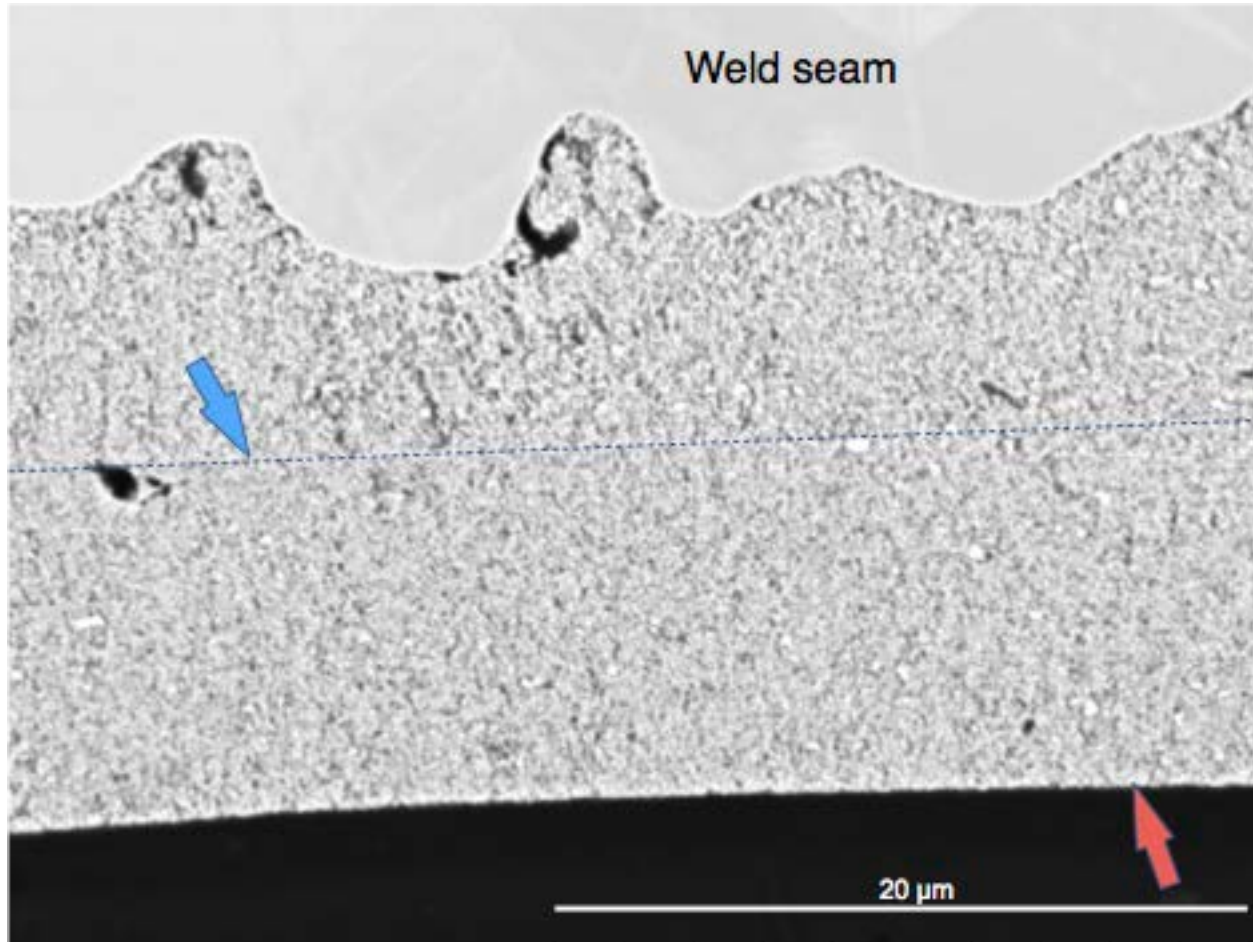
Layer thickness derived from SEM (Matlab® routine)



Forschungszentrum Jülich (Martin Bram, IEK-1, Paul Kant, IMVT)

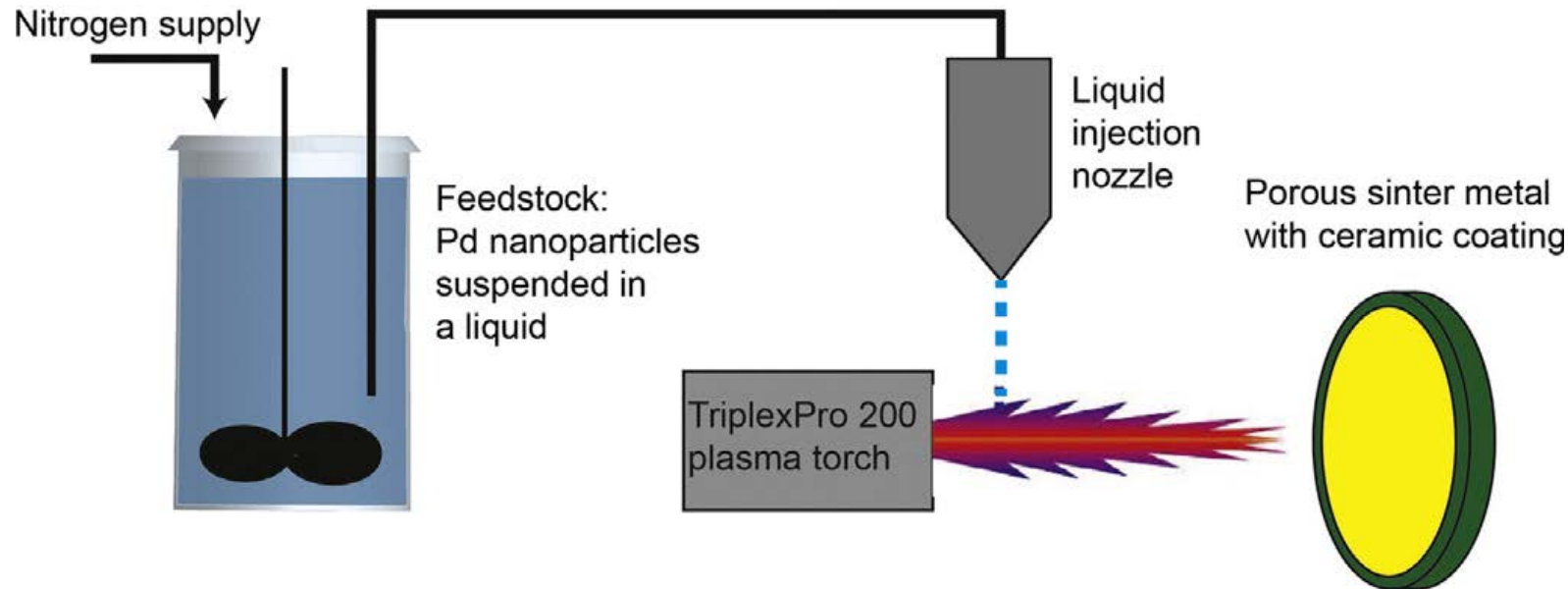


Forschungszentrum Jülich (Martin Bram, IEK-1, Paul Kant, IMVT)



Nice smooth surface for coating with thin Pd or Pd alloy layer

In cooperation with the German Aerospace Center (Sayed-Asif Ansar, Dirk Ullmer, TT, Stuttgart)



- Stable suspension of Pd nanoparticles obtained
- Injection system and plasma parameters being optimised
- First coating experiments performed on test specimen (Pd layers are not yet gastight)
- Transfer to membrane reformer modules



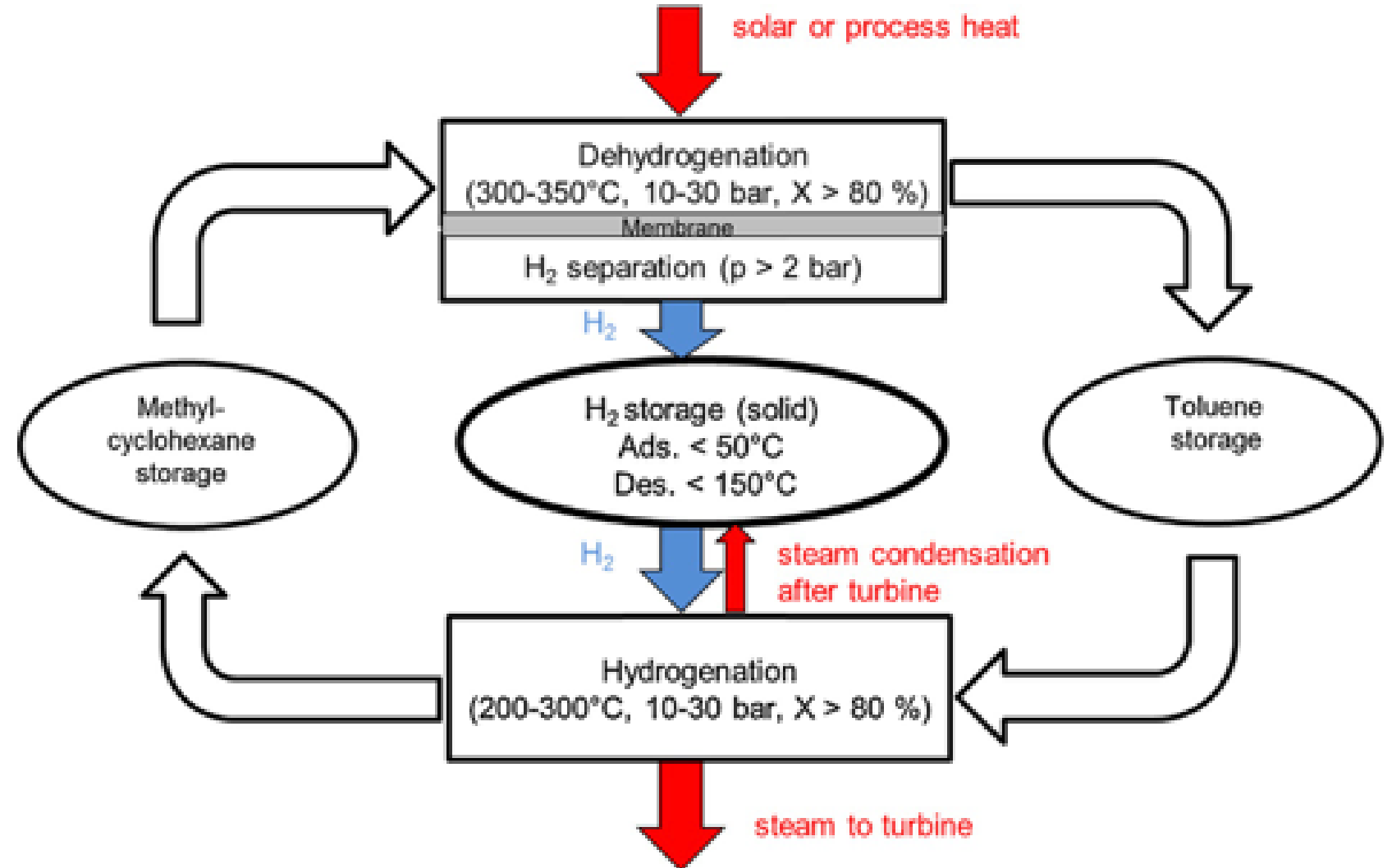
## Application background

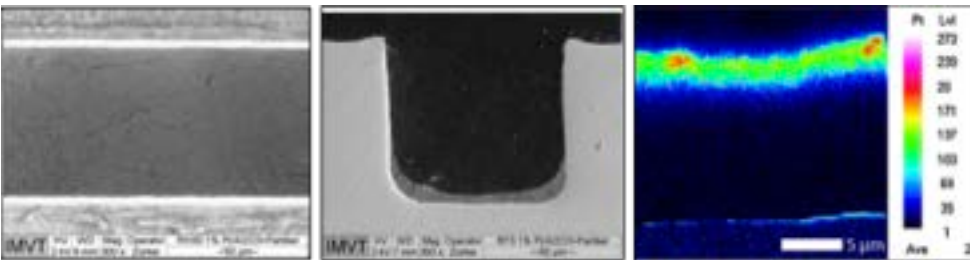
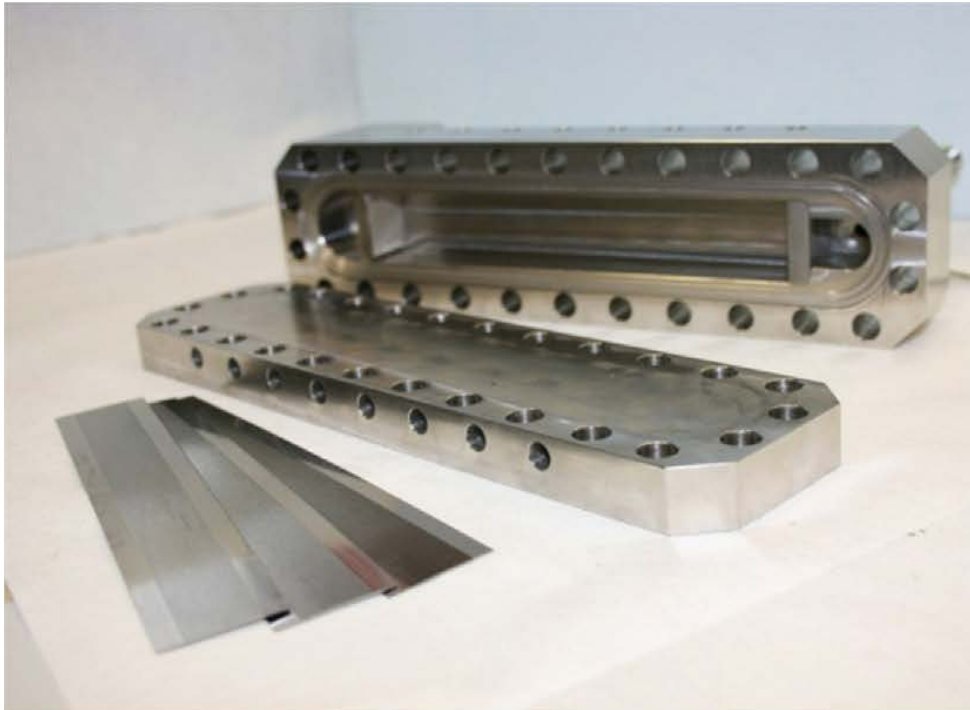
Liquid organic reaction cycle (LORC) for long-term storage of intermediate temperature heat

MCH dehydrogenation to toluene:



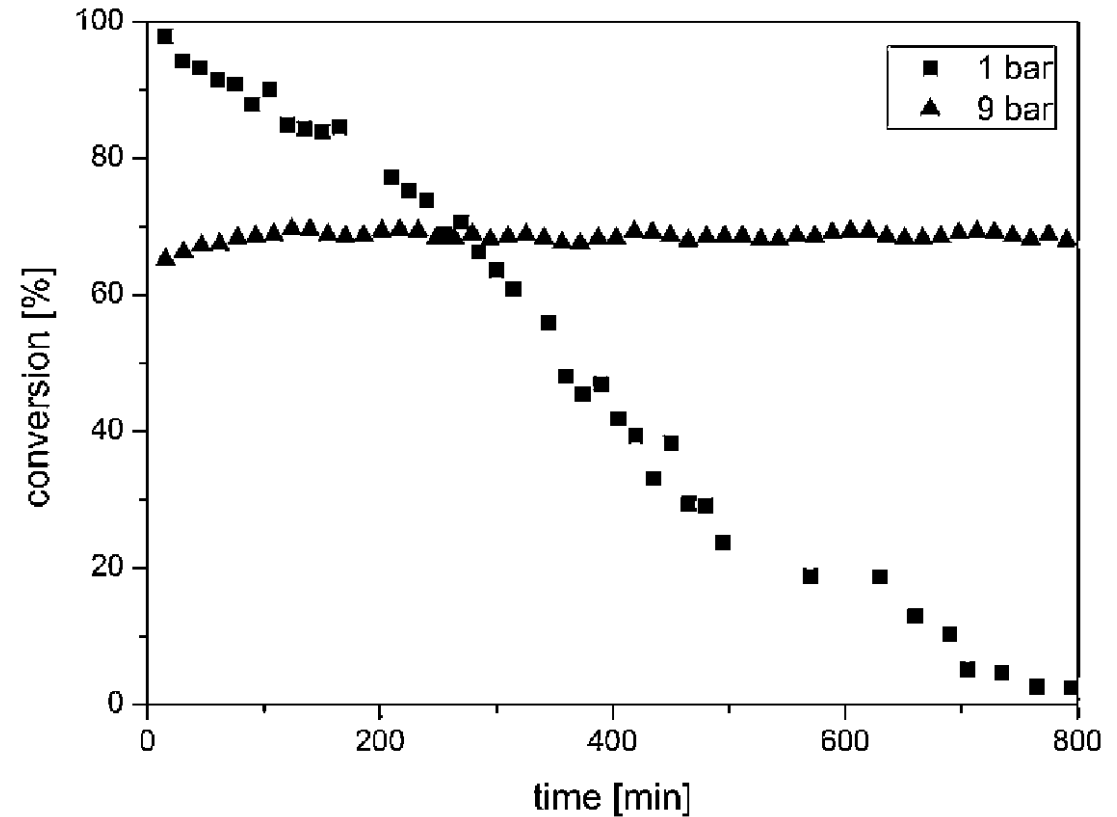
Catalyst: 1 wt.-% Pt/ $\gamma$ -Al<sub>2</sub>O<sub>3</sub>



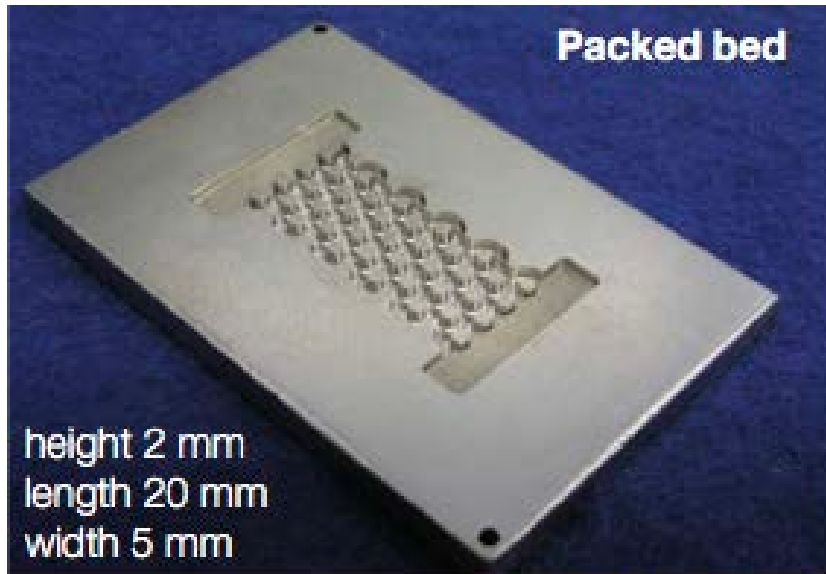


### Influence of pressure on the deactivation rate.

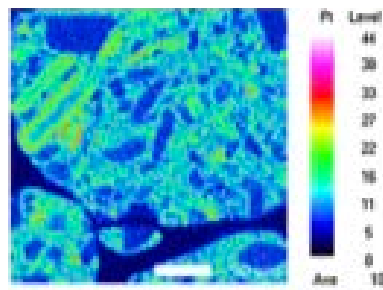
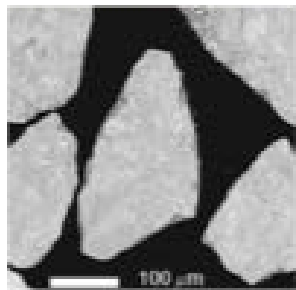
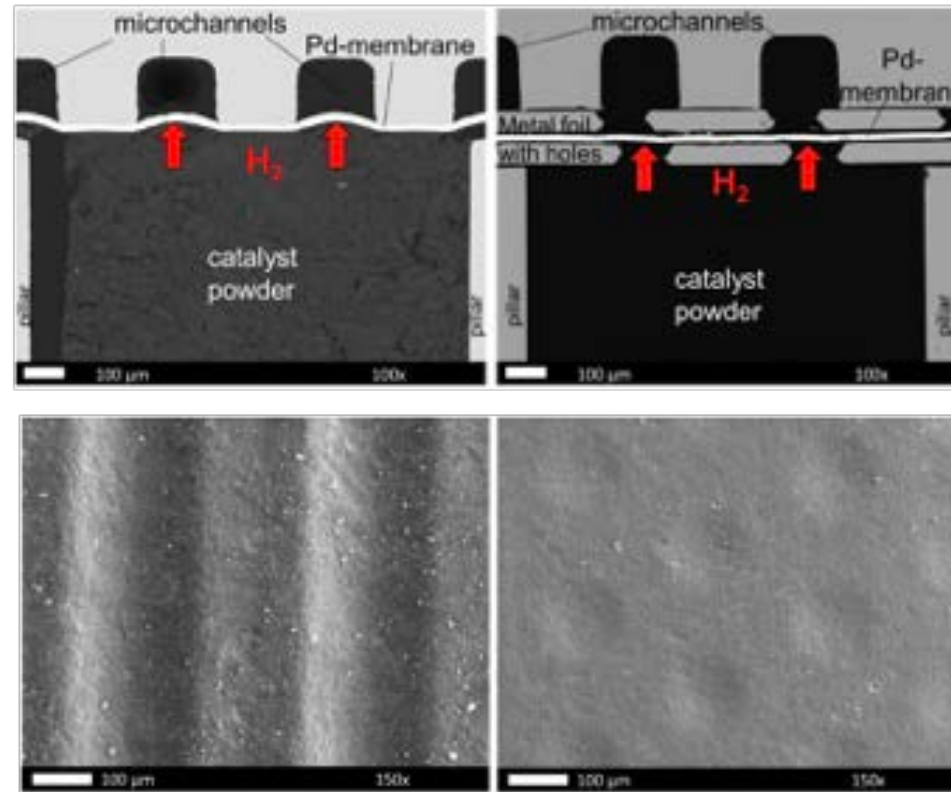
T = 325° C. modified contact time W/F 4000 kg s m<sup>-3</sup> (1 bar) and 750 kg s m<sup>-3</sup> (9 bar). MCH/N<sub>2</sub> 50/50.



- Kinetic studies in BERTY-type recycle reactor showed much slower deactivation by carbon formation



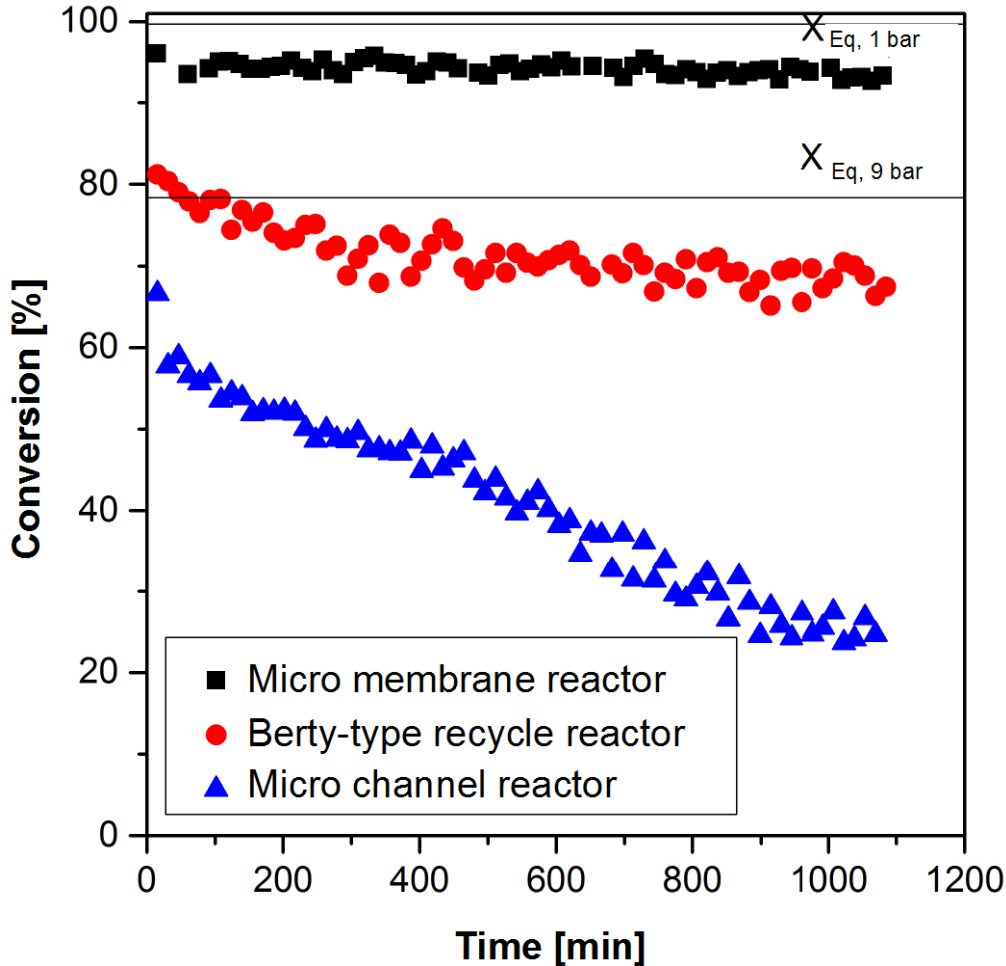
**Packed-bed and permeate sections**



Module	$Q_0 \text{ mol}\cdot\text{m}^{-1}\cdot\text{s}^{-1}\cdot\text{Pa}^{-0.5}$	$E_a \text{ kJ}\cdot\text{mol}^{-1}$	$Q (350 \text{ }^\circ\text{C}) \text{ mol}\cdot\text{m}^{-1}\cdot\text{s}^{-1}\cdot\text{Pa}^{-0.5}$	S-
membrane B	$2.8\cdot 10^{-7}$	14.6	$1.7\cdot 10^{-8}$	>3000
membrane C	$2.0\cdot 10^{-6}$	26.7	$1.1\cdot 10^{-8}$	>25,000
membrane D	$3.7\cdot 10^{-7}$	16.8	$1.5\cdot 10^{-8}$	>85,000
Boeltken et al. [18]	$2.6\cdot 10^{-7}$	14.6	$1.6\cdot 10^{-8}$	>30,000

# CATALYST DEACTIVATION BY COKING

Effect of hydrogen on deactivation.  $W/F = 250 \text{ kg s m}^{-3}$ .



350° C, 9 bar  
back permeation of H<sub>2</sub> in  
entrance region

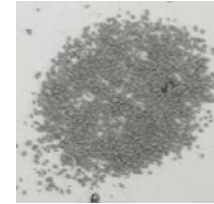
348° C, 1 bar  
perfect back mixing, i.e., H<sub>2</sub>  
concentration at reactor effluent level

400° C, 9 bar  
no back mixing, i.e., low H<sub>2</sub> partial  
pressure in entrance region

fresh



after use



Carbon content stable around 0.8 wt.-% (TGA, 400° C, BERTY reactor, up to 25 h)



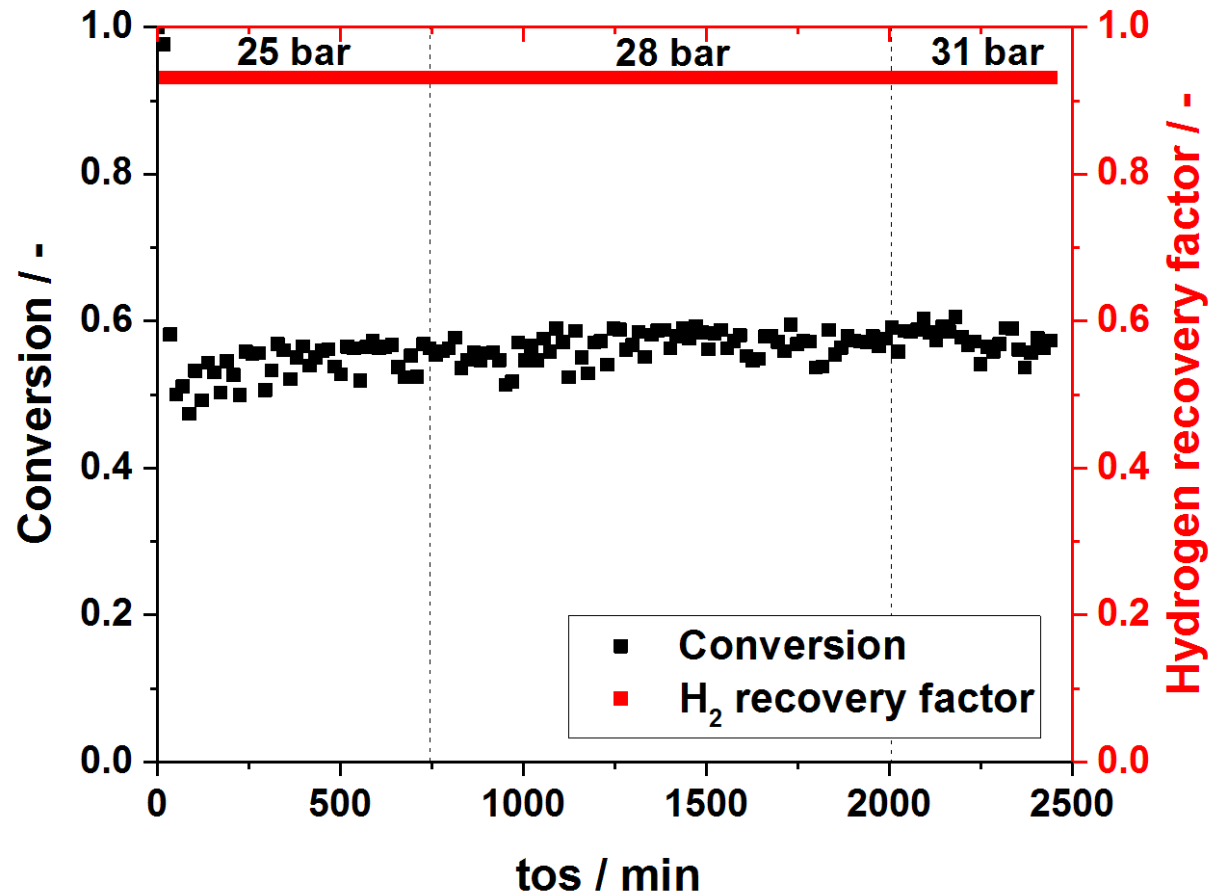
## Procedure

- 1 h treatment in a flow of 5 ml/min air plus 50 ml/min N<sub>2</sub> for during off the deposits
- 1 h treatment in a flow of 50 ml/min H<sub>2</sub> for reduction of the catalyst surface

T = 400° C.  
P<sub>Ret</sub> = 9 bar.  
W/F = 250 kg·s·m<sup>-3</sup>.  
X<sub>Eq.</sub> = 99%.



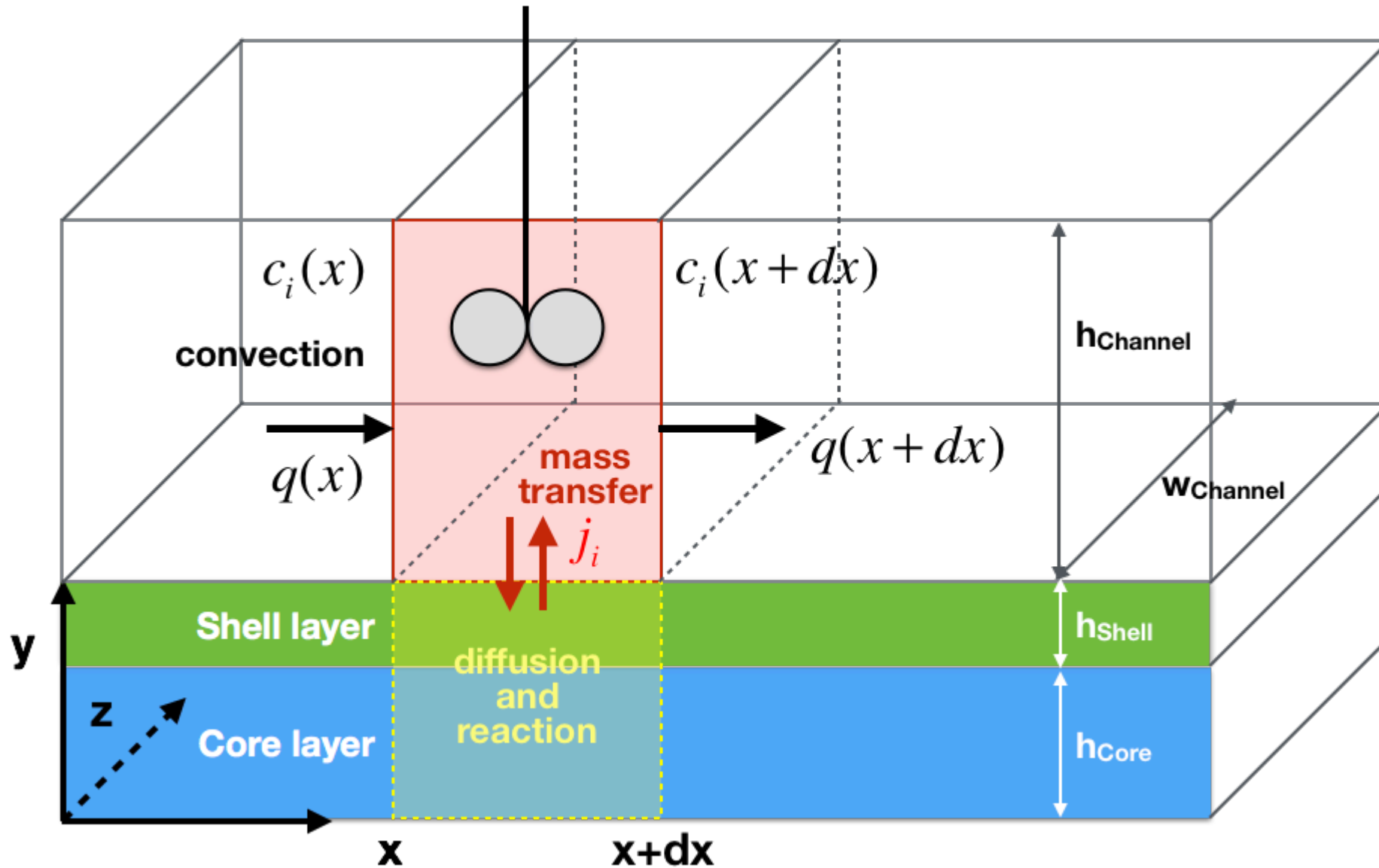
Reduced bed height of 0.5 mm / enlarged area

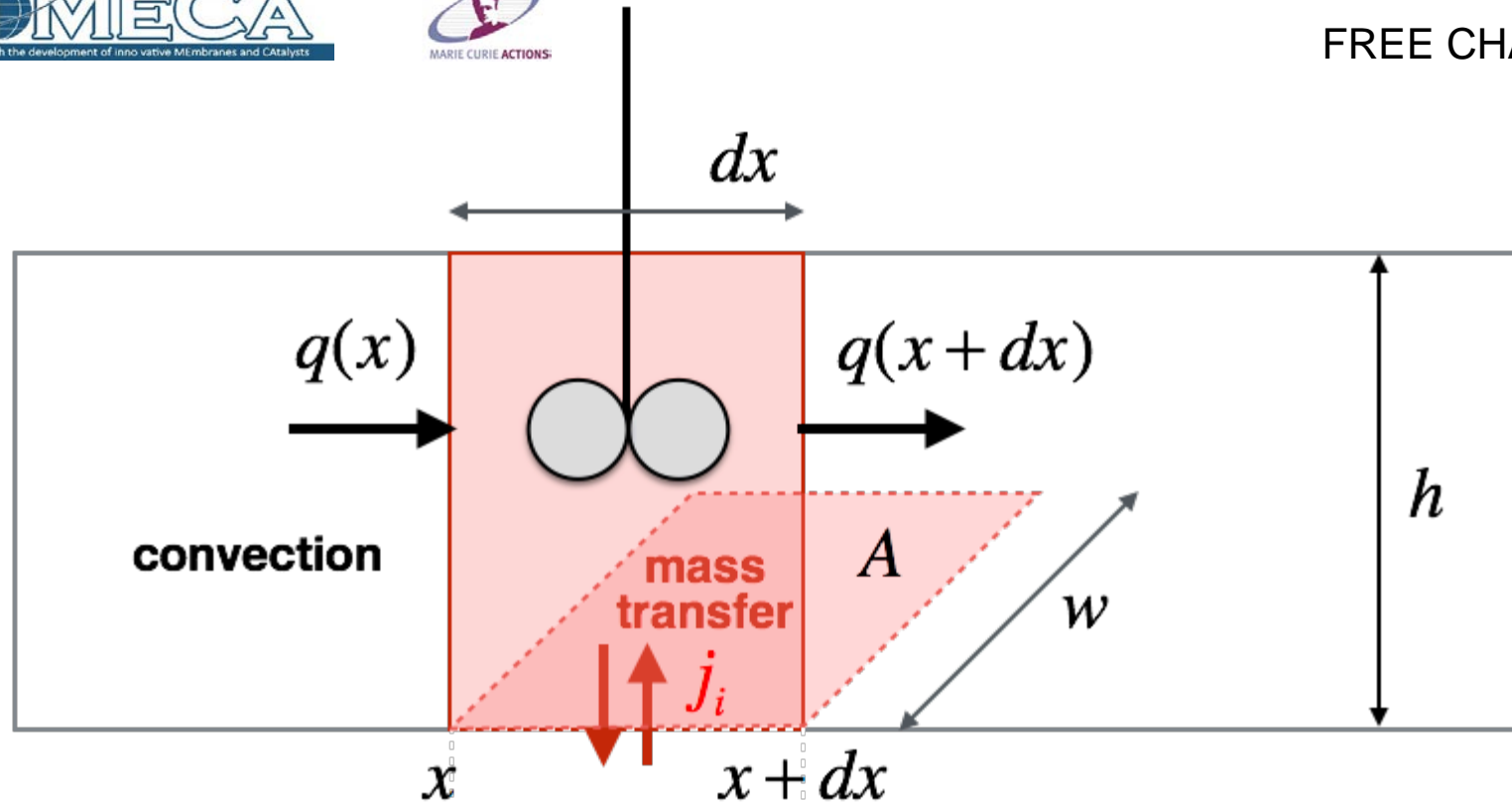


### On-going work:

- Further optimisation of reactor geometry based on simulations (optimised bed height, longer packed bed section).
- Catalyst improvement regarding coking.
- Scale-up and test in integrated process.

$T = 350^{\circ} \text{C}$ .  $P_{\text{Ret}} = 28\text{-}31 \text{ bar}$ .  $W/F = 125 \text{ kg}\cdot\text{s}\cdot\text{m}^{-3}$ .





CSTR material balance for component  $i$ :

$$0 = q(x) \cdot c_i(x) - q(x+dx) \cdot c_i(x+dx) + j_i(x+dx) \cdot A$$

$$0 = [u(x) \cdot c_i(x) - u(x+dx) \cdot c_i(x+dx)] \cdot w \cdot h + k_{ig} \cdot (c_i^*(x+dx) - c_i(x+dx)) \cdot w \cdot dx$$



new flow velocity  $u(x+dx)$  for ideal gas  
and constant pressure:

$$u(x+dx) \cdot w \cdot h = u(x) \cdot w \cdot h + \underbrace{\left[ \sum_i k_{ig} \cdot (c_i^*(x+dx) - c_i(x+dx)) \right]}_{\text{total molar flux to/from layer}} \cdot w \cdot dx \cdot \frac{RT}{p}$$

total volume flow to/from layer

$$u(x+dx) = u(x) + \frac{dx}{h} \cdot \frac{RT}{p} \sum_i k_{ig} \cdot (c_i^*(x+dx) - c_i(x+dx))$$

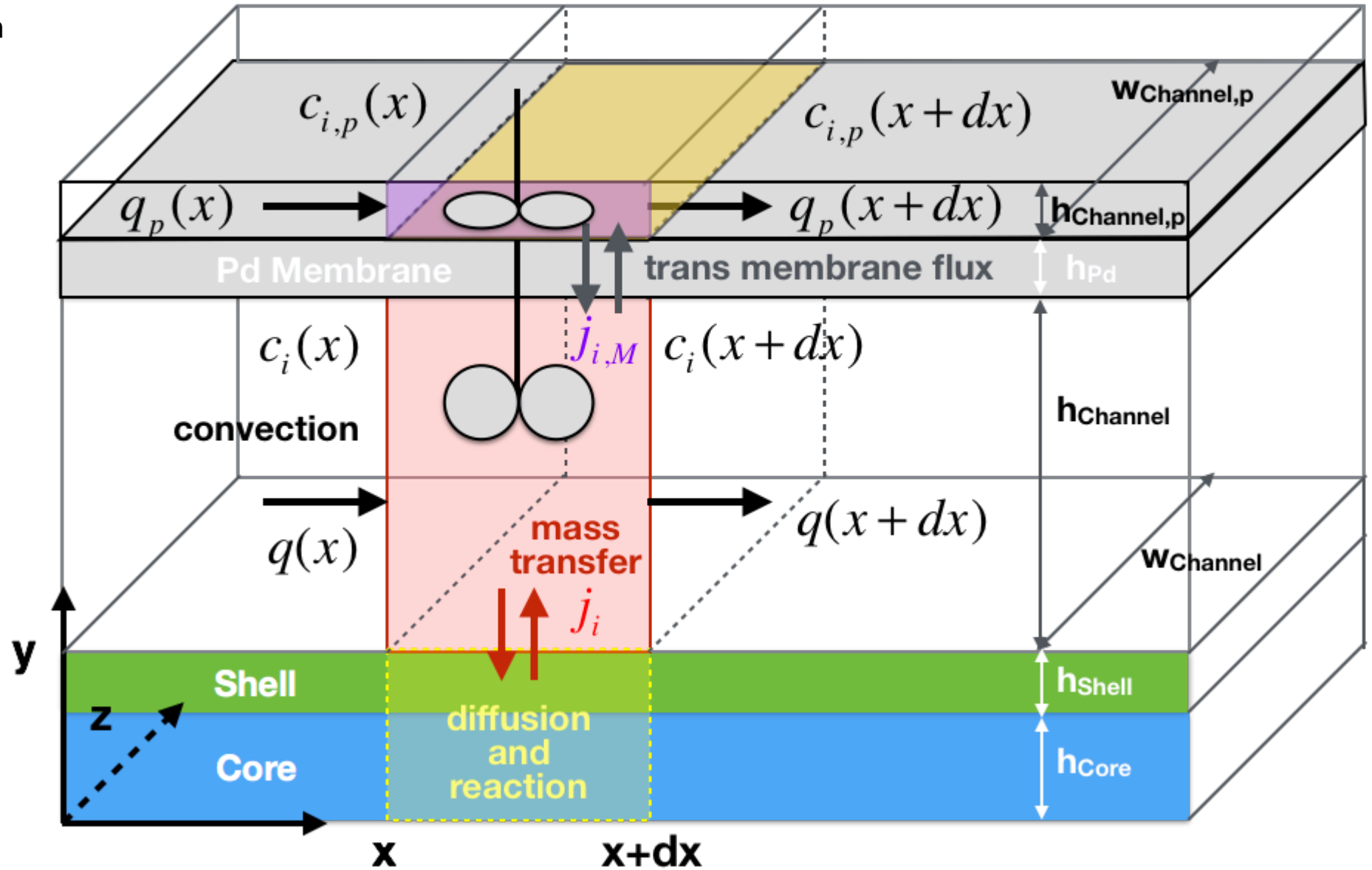
in material balance:

$$0 = u(x) \cdot [c_i(x) - c_i(x+dx)] - \frac{dx}{h} \cdot \frac{RT}{p} \cdot \left[ \sum_i k_{ig} \cdot (c_i^*(x+dx) - c_i(x+dx)) \right] \cdot c_i(x+dx) + \dots$$

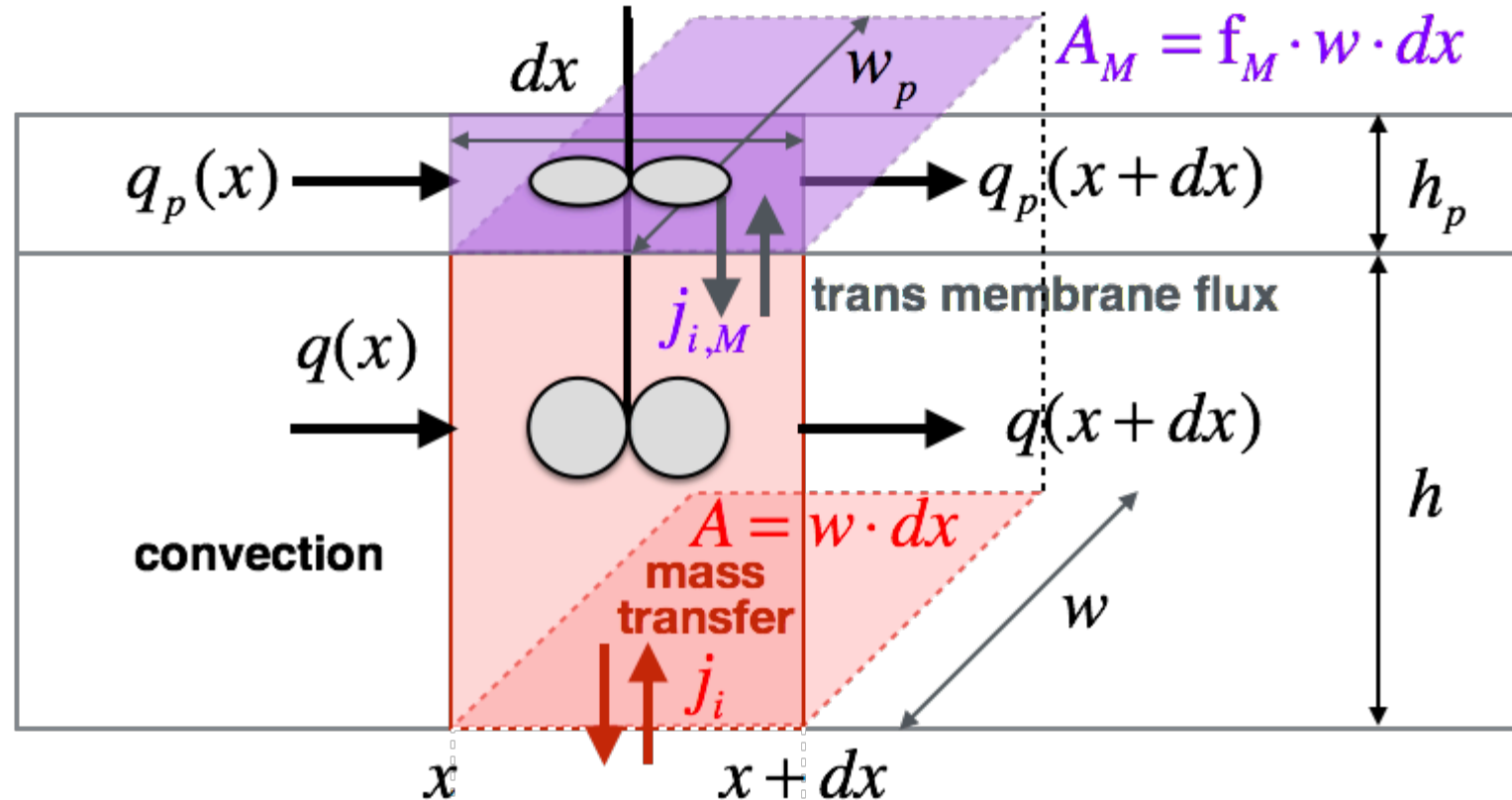
$$\dots k_{ig} \cdot (c_i^*(x+dx) - c_i(x+dx)) \cdot \frac{dx}{h}$$

concentration on the surface is given  
by reaction/diffusion inside layer

now, the situation with Pd membrane:



same approach:



CSTR material balance component  $i$  (reaction side):

$$0 = q(x) \cdot c_i(x) - q(x+dx) \cdot c_i(x+dx) + j_i(x+dx) \cdot A + j_{i,M}(x+dx) \cdot A_M$$

$$0 = [u(x) \cdot c_i(x) - u(x+dx) \cdot c_i(x+dx)] \cdot w \cdot h + k_{ig} \cdot (c_i^*(x+dx) - c_i(x+dx)) \cdot w \cdot dx + \dots$$

$$\dots j_{i,M}(x+dx) \cdot w \cdot f_M \cdot dx$$



the membrane flux connects both compartments:

$$j_{i,M}(x+dx) = -\frac{Q_{H_2}}{S_M} \cdot (RT)^{0.5} \cdot \left( c_{H_2}^{0.5}(x+dx) - c_{H_2,p}^{0.5}(x+dx) \right) \quad \text{for } i = H_2$$
$$j_{i,M}(x+dx) = 0 \quad \text{for } i \neq H_2$$

here  $j_{i,M}$  is positiv if hydrogen enters the reaction compartment via the membrane



again, new flow velocity  $u(x+dx)$  for ideal gas and constant pressure:

$$u(x+dx) \cdot w \cdot h = u(x) \cdot w \cdot h + \underbrace{\left[ \sum_i k_{ig} \cdot (c_i^*(x+dx) - c_i(x+dx)) \right]}_{\text{total molar flux to/from layer}} \cdot w \cdot dx \cdot \frac{RT}{p} + \dots$$

$$\dots - \underbrace{\frac{Q_{H_2}}{S_M} \cdot (RT)^{0.5} \cdot (c_{H_2}^{0.5}(x+dx) - c_{H_2,p}^{0.5}(x+dx)) \cdot w \cdot f_M \cdot dx \cdot \frac{RT}{p}}_{\text{total volume flow to/from permeate}}$$

$$u(x+dx) = u(x) + \frac{dx}{h} \cdot \frac{RT}{p} \cdot \left[ \sum_i k_{ig} \cdot (c_i^*(x+dx) - c_i(x+dx)) - \dots \right. \\ \left. \dots f_M \cdot \frac{Q_{H_2}}{S_M} \cdot (RT)^{0.5} \cdot (c_{H_2}^{0.5}(x+dx) - c_{H_2,p}^{0.5}(x+dx)) \right]$$

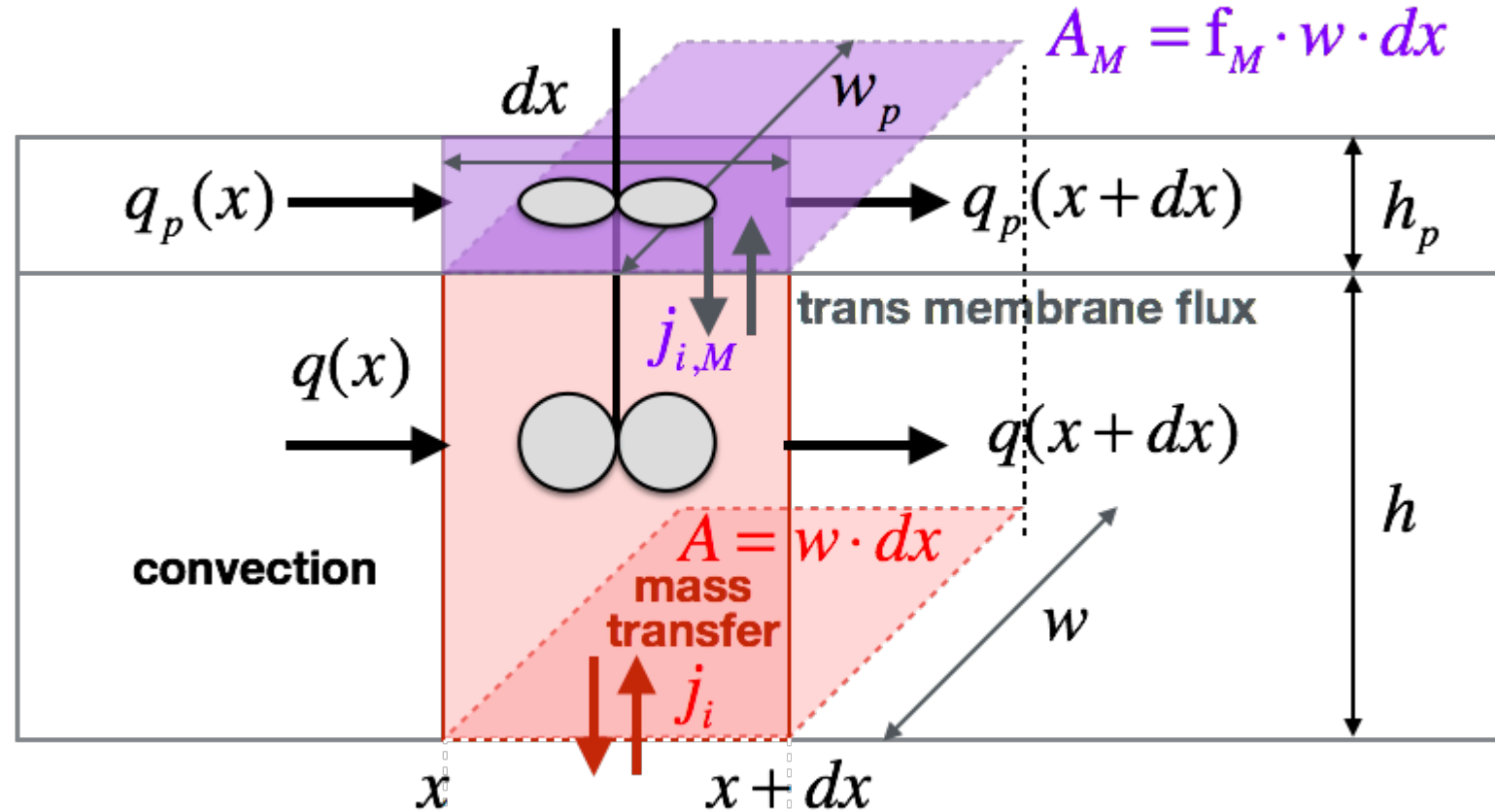


in material balance:

concentration on the surface is given by reaction/diffusion inside layer

concentration in the permeate (has to be determined by permeate side material balance)

so, permeate side:



CSTR material balance component  $i$  (permeate side):

$$0 = q_p(x) \cdot c_{i,p}(x) - q_p(x+dx) \cdot c_{i,p}(x+dx) - j_{i,M}(x+dx) \cdot A_M$$

$$0 = [u_p(x) \cdot c_{i,p}(x) - u_p(x+dx) \cdot c_{i,p}(x+dx)] \cdot w_p \cdot h_p - j_{i,M}(x+dx) \cdot w \cdot f_M \cdot dx$$



here as well, new flow velocity  $u_p(x+dx)$  for ideal gas and constant pressure:

$$u_p(x+dx) \cdot w_p \cdot h_p = u_p(x) \cdot w_p \cdot h_p + \dots$$

$$\dots \underbrace{\frac{Q_{H_2}}{S_M} \cdot (RT)^{0.5} \cdot (c_{H_2}^{0.5}(x+dx) - c_{H_2,p}^{0.5}(x+dx)) \cdot w \cdot f_M \cdot dx \cdot \frac{RT}{p}}_{\text{total volume flow to/from permeate}}$$

$$u_p(x+dx) = u_p(x) + \frac{dx}{h_p} \cdot f_M \cdot \frac{w}{w_p} \cdot \frac{(RT)^{1.5}}{p} \cdot \frac{Q_{H_2}}{S_M} \cdot [c_{H_2}^{0.5}(x+dx) - c_{H_2,p}^{0.5}(x+dx)]$$

note that pressure p here is the permeate pressure, which is in general different from the reaction side pressure

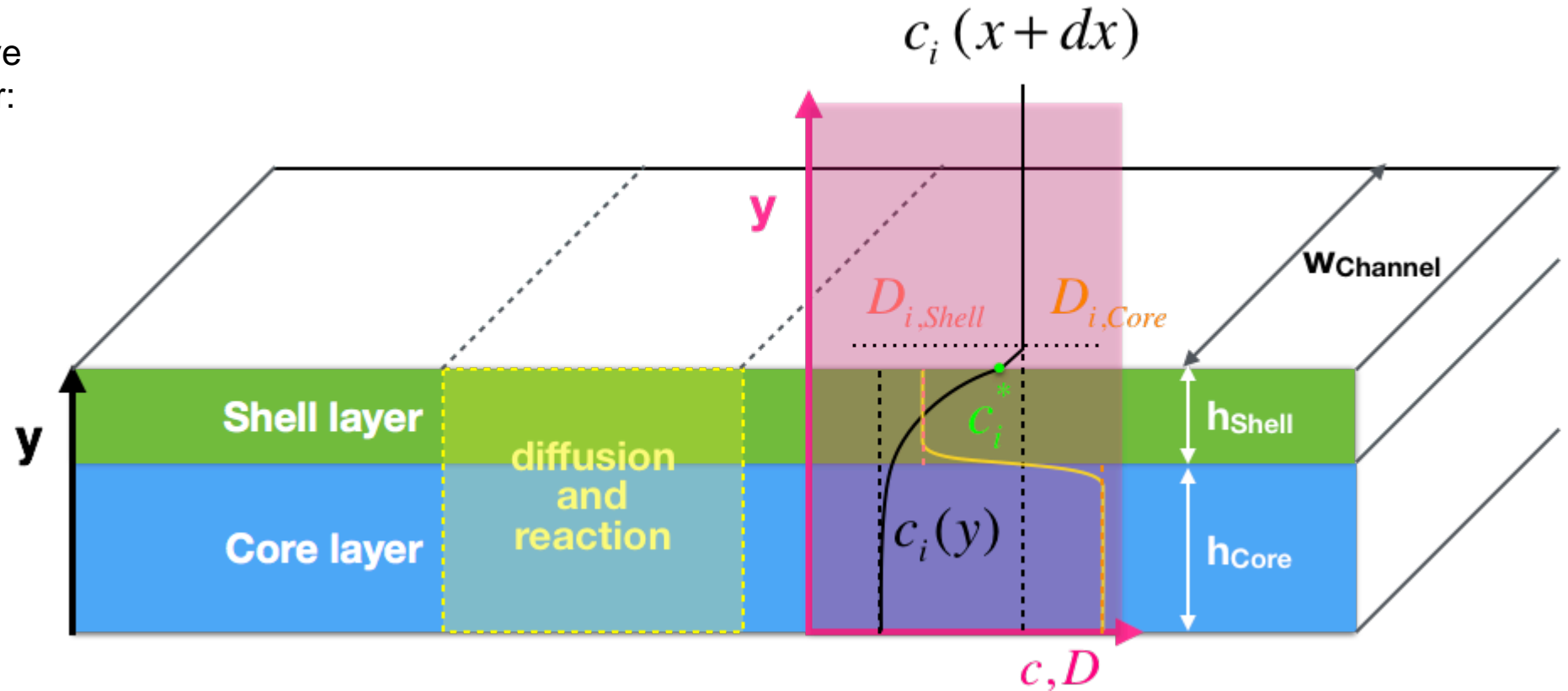


in material balance:

$$0 = u_p(x) \cdot [c_{i,p}(x) - c_{i,p}(x + dx)] + \dots$$
$$\dots \frac{dx}{h_p} \cdot f_M \cdot \frac{w}{w_p} \cdot \frac{(RT)^{1.5}}{p} \cdot \frac{Q_{H_2}}{S_M} \cdot (c_{H_2}^{0.5}(x + dx) - c_{H_2,p}^{0.5}(x + dx)) \cdot c_{i,p}(x + dx) - \dots$$
$$\dots j_{i,M} \cdot f_M \cdot \frac{dx}{h_p}$$

again, note that pressure p here is the permeate pressure, which is in general different from the reaction side pressure

now, we need to solve the ODE for the layer:

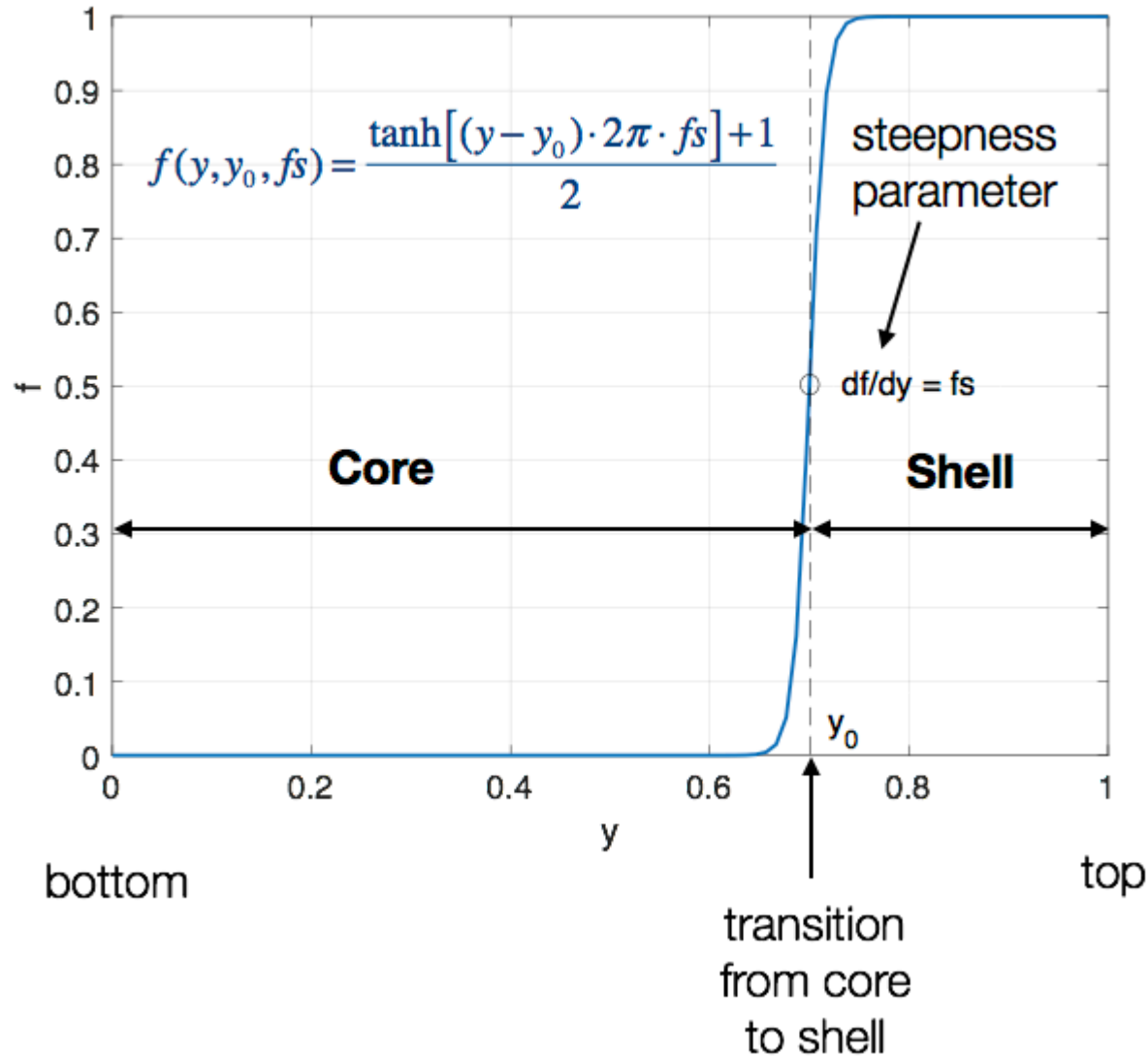


Standard ODE (constant diffusivity): 
$$0 = D_i \cdot \frac{d^2 c_i}{dy^2} + R_i(c_i, T)$$

- different diffusivities  $D_i$  in the two layers can be handled via position-dependent effective diffusivity  $D_i(y)$
- the presence of different catalysts in the two layers can also be handled via position-dependent catalyst mass concentrations  $\rho_{\text{Cat},j}(y)$



## NON-DIMENSIONAL FUNCTION F WITH 2 PARAMETERS



Effective diffusivity as step function:

$$D_i = D_{i,Core} + f(y) \cdot (D_{i,Shell} - D_{i,Core})$$

Catalyst mass concentrations as step functions:

$$\rho_{Cat,Core}(y) = [1 - f(y)] \cdot \rho_{Core}$$

$$\rho_{Cat,Shell}(y) = f(y) \cdot \rho_{Shell}$$



$$0 = \underbrace{-D_i(y) \cdot \frac{dc_i}{dy}(y) \cdot dx \cdot w}_{\text{influx}} + \underbrace{D_i(y+\Delta y) \cdot \frac{dc_i}{dy}(y+\Delta y) \cdot dx \cdot w}_{\text{outflux}} + \underbrace{\left[ \frac{R_i(y) + R_i(y+\Delta y)}{2} \right] \cdot \Delta y \cdot dx \cdot w}_{\text{source term}}$$

$$0 = -D_i \cdot \frac{dc_i}{dy} + \left[ D_i + \frac{dD_i}{dy} \cdot \Delta y \right] \cdot \left[ \frac{dc_i}{dy} + \frac{d^2c_i}{dy^2} \cdot \Delta y \right] + \left[ \frac{R_i + R_i + \frac{dR_i}{dy} \cdot \Delta y}{2} \right] \cdot \Delta y$$

$$0 = -D_i \cdot \frac{dc_i}{dy} + \left[ D_i \cdot \frac{dc_i}{dy} + \frac{dD_i}{dy} \cdot \Delta y \cdot \frac{dc_i}{dy} + D_i \cdot \frac{d^2c_i}{dy^2} \cdot \Delta y + \frac{dD_i}{dy} \cdot \frac{d^2c_i}{dy^2} \cdot (\Delta y)^2 \right] + \left[ R_i \cdot \Delta y + \frac{1}{2} \cdot \frac{dR_i}{dy} \cdot (\Delta y)^2 \right]$$

$$0 = \frac{dD_i}{dy} \cdot \frac{dc_i}{dy} + D_i \cdot \frac{d^2c_i}{dy^2} + R_i \quad \longrightarrow \quad \frac{d^2c_i}{dy^2} = -\frac{R_i(y)}{D_i(y)} - \frac{1}{D_i(y)} \cdot \frac{dD_i(y)}{dy} \cdot \frac{dc_i}{dy} \quad \text{extra term}$$



$$\frac{d^2 c_i}{dy^2} = -\frac{R_i(y)}{D_i(y)} - \frac{1}{D_i(y)} \cdot \frac{dD_i(y)}{dy} \cdot \frac{dc_i}{dy}$$

where: 
$$\frac{dD_i(y)}{dy} = (D_{i,core} - D_{i,shell}) \cdot \frac{df}{dy}$$

and: 
$$\frac{df}{dy} = \frac{df}{dy' \cdot s} = \frac{1}{s} \cdot \left(1 - \tanh^2 \left[ (y - y_0) \cdot 2\pi \cdot f_s \right] \right) \cdot \pi \cdot f_s$$

due to:

$$s = h_{core} + h_{shell}$$

$$y = \frac{y'}{s}$$

$$y_0 = \frac{h_{core}}{s}$$



$$\frac{d^2 c_i}{dy^2} = -\frac{R_i(y)}{D_i(y)} - \frac{1}{D_i(y)} \cdot \frac{dD_i(y)}{dy} \cdot \frac{dc_i}{dy}$$

Boundary conditions:

$y=0$	$y=h_{\text{Core}}+h_{\text{Shell}}$
$\left. \frac{dc_i}{dy} \right _{y=0} = 0$	infinite mass transfer rate
	finite mass transfer rate

concentration in bulk phase

$$c_i \Big|_{y=h_{\text{Core}}+h_{\text{Shell}}} = c_i(x+dx)$$

$$D_{i,\text{Shell}} \cdot \left. \frac{dc_i}{dy} \right|_{y=h_{\text{Core}}+h_{\text{Shell}}} = k_{ig} \cdot \left( c_i(x+dx) - c_i^*(x+dx) \right)$$

concentration on top of double layer



Case 1: infinite mass transfer rate

$$c_i \Big|_{y=h_{\text{Core}}+h_{\text{Shell}}} = c_i(x+dx)$$

flux from/to layer is expressed with the concentration gradient at top of the double layer

$$0 = u(x) \cdot [c_i^*(x) - c_i(x+dx)] - \frac{dx}{h} \cdot \frac{RT}{p} \cdot \left[ \sum_i k_{ig} \cdot (c_i^*(x+dx) - c_i(x+dx)) - \dots \right. \\
\left. \dots f_M \cdot \frac{Q_{H_2}}{S_M} \cdot (RT)^{0.5} \cdot (c_{H_2}^{0.5}(x+dx) - c_{H_2,p}^{0.5}(x+dx)) \right] \cdot c_i(x+dx) + \dots \\
\dots k_{ig} \cdot (c_i^*(x+dx) - c_i(x+dx)) \cdot \frac{dx}{h} + j_{i,M} \cdot f_M \cdot \frac{dx}{h}$$

where:  $k_{ig} \cdot (c_i^*(x+dx) - c_i(x+dx)) = -D_{i,Shell} \cdot \frac{dc_i}{dy} \Big|_{y=h_{\text{Core}}+h_{\text{Shell}}}$

$$\begin{aligned}
 0 = & u(x) \cdot [c_i(x) - c_i(x + dx)] - \frac{dx}{h} \cdot \frac{RT}{p} \cdot \left[ \sum_i -D_{i,Shell} \cdot \frac{dc_i}{dy} \Big|_{y=h_{Core}+h_{Shell}} - \dots \right. \\
 & \left. \dots f_M \cdot \frac{Q_{H_2}}{S_M} \cdot (RT)^{0.5} \cdot (c_{H_2}^{0.5}(x + dx) - c_{H_2,p}^{0.5}(x + dx)) \right] \cdot c_i(x + dx) - \dots \\
 & \dots D_{i,Shell} \cdot \frac{dc_i}{dy} \Big|_{y=h_{Core}+h_{Shell}} \cdot \frac{dx}{h} + j_{i,M} \cdot f_M \cdot \frac{dx}{h}
 \end{aligned}$$

rearranging:

$$c_i \Big|_{y=h_{Core}+h_{Shell}} = c_i(x + dx) = \frac{u(x) \cdot c_i(x) - \frac{dx}{h} \cdot \left[ D_{i,Shell} \cdot \frac{dc_i}{dy} \Big|_{y=h_{Core}+h_{Shell}} - j_{i,M} \cdot f_M \right]}{u(x) - \frac{dx}{h} \cdot \frac{RT}{p} \cdot \left[ \sum_i D_{i,Shell} \cdot \frac{dc_i}{dy} \Big|_{y=h_{Core}+h_{Shell}} + f_M \cdot \frac{Q_{H_2}}{S_M} \cdot (RT)^{0.5} \cdot (c_{H_2}^{0.5}(x + dx) - c_{H_2,p}^{0.5}(x + dx)) \right]}$$

- $c_{H_2,p}(x+dx)$  is found from the hydrogen material balance for permeate side for given sweep gas flow rate, permeate pressure and reaction side hydrogen concentration.
- owing to Sievert's law this requires the solution of a nonlinear equation.



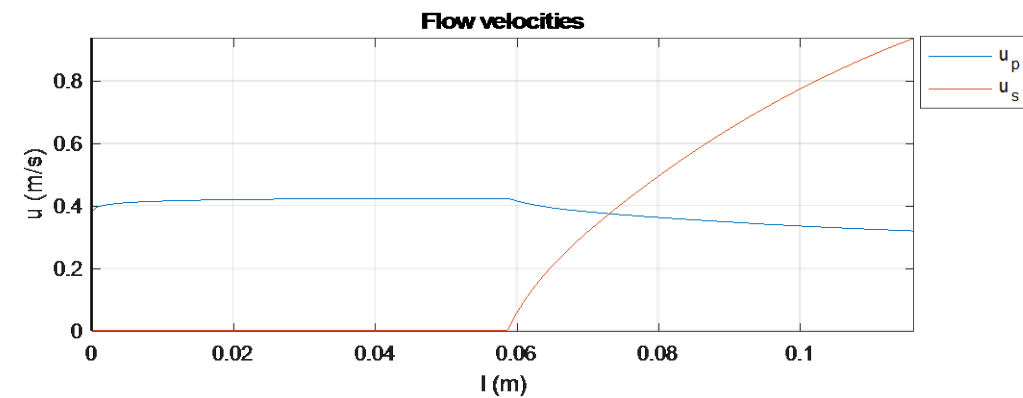
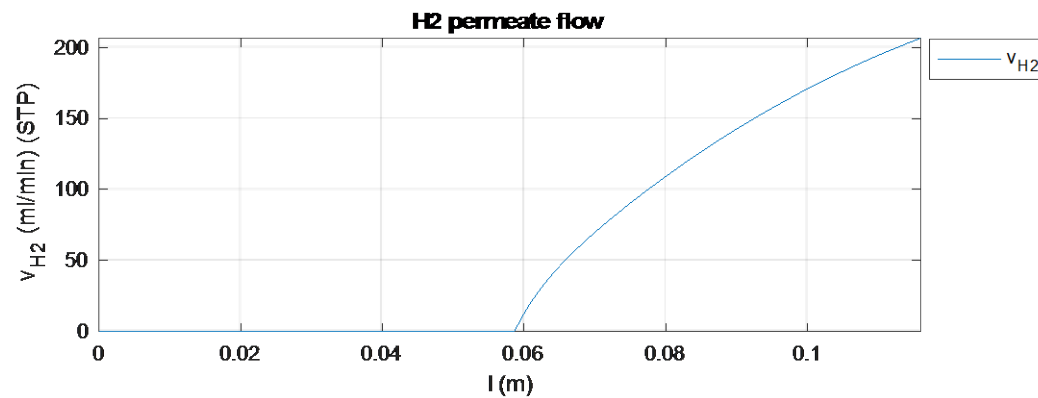
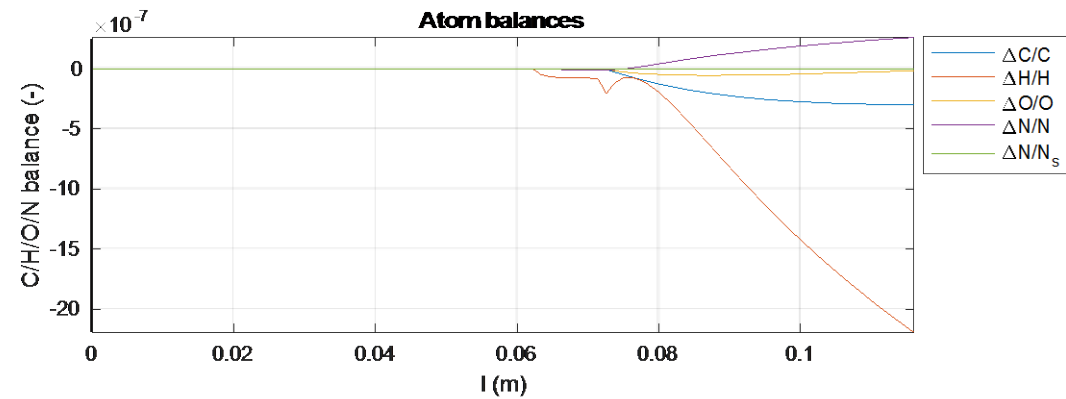
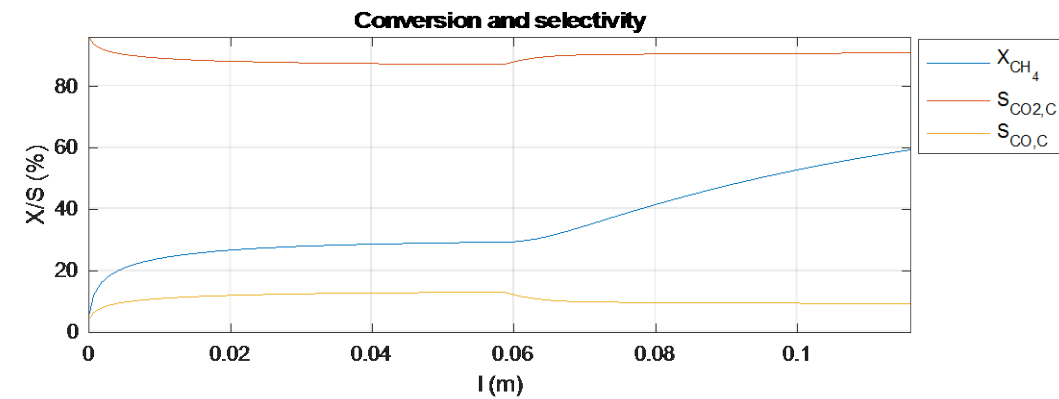
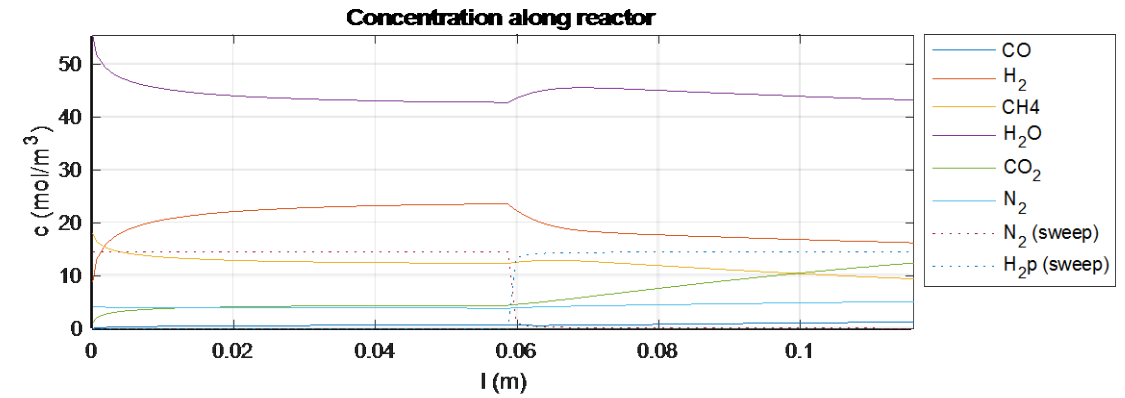
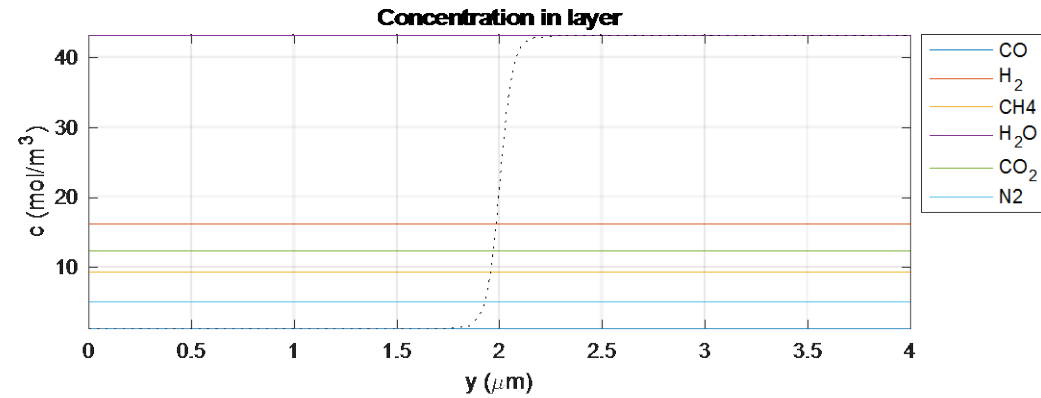
### **Flexible approach - 1D cascade of cells with the option to limit the concentration change per cell via step size control**

- solved profiles for one cell are used as initial guess for subsequent cell
- mole flows in both compartments are updated based on solved profiles
- graphics for monitoring progress of the calculation
- material balance checks
- heat balance not yet implemented
- pressure drop along channel neglected

### **bvp4c - reliable boundary value problem solver with adaptive grid**

- CSTR material balance and membrane transport integrated in the definition of the boundary conditions
- nonuniform catalyst distribution and effective diffusivity - two distinct layers approximated by S-shaped distribution function

### **Exchangeable kinetics and permeation**





First commercial applications of membrane reactors may appear in

- small-capacity hydrogen production for industrial uses via on site reforming (low pressure, moderate purity),
- hydrogen generation from LOHC in the context of hydrogen logistics,

rather than in large-scale reforming or WGS.

- Transport effects may have a big influence on reactor performance (yield, selectivity, space time yield, etc.); this holds especially for membrane reactors where the reactions kinetics should not only match the usual heat and mass transport rates but also the permeation kinetics.
- Matlab is a flexible platform for building your own customised models for „multiscale“ reactor simulation



- Financial support by the Helmholtz Research School „Energy-Related Catalysis“ in the frame of a PhD scholarship.
- Financial support by Helmholtz Association and CAS for joint research group 118 „Integrated catalytic technologies for efficient hydrogen production“.
- The German Federal Ministry of Education and Research for financial support in the frame of the Kopernikus project „Power to X“.
- All colleagues at IMVT for their dedication and professional work.

SPONSORED BY THE



Federal Ministry  
of Education  
and Research



*Thank you for your attention*

FOR MORE INFORMATION:  
[roland.dittmeyer@kit.edu](mailto:roland.dittmeyer@kit.edu)